Mechanical properties of bioactive glasses, ceramics, glass-ceramics and composites: State-of-the-art review and future challenges

Mechanical properties of bioactive glasses, ceramics, glass-ceramics and composites: state-of-the-art review and future challenges

Gurbinder Kaur[*a], Vishal Kumar[b], Francesco Baino[c], John C. Mauro[d], Gary Pickrell[e], Iain Evans[f], Oana Bretcanu[f]

[a]School of Physics and Materials Science, Thapar University, Patiala-147001, India
[b]Shri Guru Granth Sahib World University, Fatehgarh Sahib, 140406, India
[c]Applied Science and Technology Department (DISAT), Politecnico di Torino, 10129 Turin, Italy
[d] College of Earth and Mineral Sciences, The Pennsylvania State University, PA-16802, USA
[e] Material Science and Engineering, Virginia Tech, VA-24060, USA.
[f] School of Engineering, Newcastle University, Newcastle upon Tyne, NE1 7RU, UK

Corresponding author: Gurbinder Kaur

E-mail address: gkapds@gmail.com

Telephone no.: +91-98883-72281

Table of Contents

Abstract

The repair and restoration of bone defects in orthopaedic and dental surgery remains a major challenge despite advances in surgical procedures and post-operative treatments. Bioactive glasses, ceramics, glass-ceramics and composites show considerable potential for such applications as they can promote bone tissue regeneration. This paper presents an overview of the mechanical properties of various bioactive materials, which have the potential for bone regeneration. It also identifies current strategies for improving the mechanical properties of these novel materials, as these are rarely ideal as direct replacements for human bone. For this reason bioactive organic-inorganic composites and hybrids that have tailorable mechanical properties are of particular interest. The inorganic component (bioactive glass, ceramic or glass-ceramic) can provide both strength and bioactivity, while the organic component can add structural reinforcement, toughness and processability. Another topic presented in this paper includes 3D porous scaffolds that act as a template for cell attachment, proliferation and bone growth. Mechanical limitations of existing glass and ceramic scaffolds are discussed, along with the relevant challenges and strategies for further improvement. Advantages and disadvantages of different bioactive materials are critically examined. This paper is focused on optimization of biomaterials properties, in particular mechanical properties and bioactivity.

1. Introduction

Glasses are amorphous solids, which lack long-range structural order and exhibit open structure [1, 2, 3]. Bioactive glasses were introduced in the early 1970s by Larry Hench and the first commercialized glass was named Bioglass® 45S5 [4, 5]. Bioactive glasses are excellent materials for clinical applications due to their high biocompatibility and bioactivity. Bioactive glasses, as well as some crystalline ceramics like hydroxyapatite (HA) and tricalcium phosphate (TCP), are osteoconductive and bond to the bone without any fibrous

connective tissue interface [5, 6, 7, 8]. Upon implantation of bioactive glasses into the defect site, ion exchange reactions take place between the glass surface and the surrounding biological fluid, leading to the formation of a bone-like apatite layer on the implant surface. This biological apatite is partially replaced by the bone after long-term implantation because apatite promotes cellular adhesion and proliferation of osteogenic cells [9, 10, 11].

Despite the excellent bioactive properties, the major disadvantages of bioactive glasses and ceramics are their low mechanical strength and fracture toughness. These characteristics typically restrict their use to non-load bearing applications. However, smart strategies like combination with polymeric phases to produce composites or development of novel fabrication methods (e.g. additive manufacturing techniques) allow partial overcoming of these drawbacks. The present review focuses on the mechanical properties of bioactive glasses, ceramics, glass-ceramics and composite materials for orthopaedic applications, providing a picture of the current state of the art and highlighting open issues and challenges for the near future.

2. Mechanical properties of bioactive glasses

Ideally, bioactive implants for clinical applications should match the mechanical properties of the host tissue and exhibit strong interfacial bonds with hard and/or soft tissues [12, 13, 14, 15, 16, 17, 18, 19]. Given the inorganic nature and mechanical properties of bioactive glasses, which possess physical characteristics relatively close to ‘hard’ bone tissue, great attention has been focused on using these biomaterials in contact with bone and teeth. The main mechanical properties of some commercial bioactive glasses and glass-ceramics, hydroxyapatite and human bones are summarised in Table 1. All the synthetic materials listed in Table 1 exhibit notably lower toughness than natural load-bearing cortical bone.

Table 1 Mechanical properties of bioactive glasses, ceramics and human bones [20, 21, 22, 23] (HA = hydroxyapatite; AW = apatite wollastonite)

Material	Compressive modulus (GPa)	Compressive strength (MPa)	Fracture toughness (MPa $m^{1/2}$)	Bending strength (MPa)	Vickers Hardness (MPa)	Structure
HA	35-120	100-150	0.8-1.2	60-120	90-140	ceramic
Bioglass® 45S5	60	-	0.6	40	-	glass
Bioglass® 52S4.6	60	-	-	40	-	glass
Cerabone® AW	120	1080	2	215	680	glass-ceramic
Ceravital®	100-160	500	-	100-150	-	glass-ceramic
Bioverit® I	70-90	500	1.2–2.1	140-180	-	glass-ceramic
Bioverit® II	70	450	1.2–1.8	90-140	-	glass-ceramic
Bioverit® III	45	-	0.6	60-90	-	glass-ceramic
Trabecular bone	0.05–0.6	1.5-7.5	0.1-0.8	10-20	40-60	-
Cortical bone	7–30	100-135	2–12	50-150	60-75	-

The fracture toughness values obtained for $CaO\text{-}Al_2O_3\text{-}P_2O_5$ glasses are in the range 0.2-0.6 MPa•$m^{1/2}$, which are similar to the fracture toughness of trabecular bone (0.1-0.8MPa•$m^{1/2}$), but are much lower than the values for cortical bone (2-12 MPa•$m^{1/2}$) [24, 25, 26, 27].

More details on the bioactive glass products in current clinical use for healthcare can be found elsewhere [28, 29].

3. Mechanical properties of bioactive glass-ceramics

Upon high-temperature thermal treatment, bioactive glasses can partially crystallize, originating glass-ceramic materials with superior mechanical properties compared to the parent glass. Glass-ceramics possess crystalline phases embedded in a residual amorphous matrix. The crystalline phases enhance the strength of glass-ceramics and give them higher fracture toughness when compared to the parent glass. In this regard, crack bridging and crack deflection were determined to be the most potent toughening mechanisms [30, 31, 32,

33, 34, 35]. The main properties and applications of bioactive glass-ceramics for use in orthopaedics and dentistry have been recently reviewed by Montazerian and Zanotto [36].

Table 1 indicates that the glass-ceramic Cerabone® AW ($34SiO_2$–$16.2P_2O_5$–44.7CaO–$0.5CaF_2$–4.6MgO wt%) [22, 37] has higher mechanical properties than 45S5 Bioglass and hydroxyapatite HA. Therefore, apatite-wollastonite (AW) glass-ceramic is used for vertebral replacements where significant compressive strength is required [38].

The major concern when using partially crystallized glasses is the corresponding decrease in bioactivity, as ion-exchange phenomena at the interface between implant surface and biological fluids are mainly related to the residual glassy phase. Hench and co-workers found that 40% crystallinity did not affect the bioactivity of partially crystallized 45S5 Bioglass®. However, the formation rate for an apatite layer at a surface is slowed down if crystallinity reaches 100%, although it is not totally suppressed [39]. Kokubo and co-workers reported that AW glass-ceramics did not form a HA layer when immersed in Tris-buffer solution. However, the formation of a polycrystalline HA layer occurred on their surface upon soaking in the simulated body fluid (SBF) [33, 34].

Bioactive glass-ceramics in the MgO-CaO-SiO_2-P_2O_5 system, containing apatite and β-wollastonite phases can be obtained by sintering and subsequent crystallization of glass powders. Increasing the P_2O_5 content results in a decrease in compressive strength [40].

Bending strength and Vickers microhardness tests were performed on glass-ceramic samples obtained by sintering of bioactive glasses containing MgF_2 and MgO [41]. Glasses with the composition (50-x) CaO–$34SiO_2$–$14.5P_2O_5$–CaF_2–$0.5MgF_2$– x MgO (wt. %) (where x = 4, 25 and 46) were synthesized by a conventional melt-quenching method. The glass samples were formed into pellets in a hydraulic press and then sintered in two steps, at temperatures between 700-735 ^oC for 1h (for step1) and 950-990 ^oC for 3h (for step2). Increasing the MgO content resulted in an increase in the sintering temperature [41]. The

resultant glass-ceramic samples had Vickers microhardness of 4.9-6.9 (GPa) and bending strength of 210-280 MPa. These values increased with the increase of the MgO content in the parent glass composition [41].

Glass-ceramics were prepared by sintering a melt-derived bioactive glass with the mol% composition $33SiO_2$-21CaO-$32.5Na_2O$-$12P_2O_5$-1.5MgO, at three different temperatures 750 ^oC, 800 ^oC, and 850 ^oC [42]. Vickers hardness tests performed on glass ceramic samples showed an increase of hardness values with the sintering temperature from 5.6 to 7.1 (GPa). As expected, increasing the sintering temperature the structure will become denser, porosity will decrease and crystallinity will increase, leading to enhanced mechanical properties [42].

Al-Haidary et al showed that the addition of 0.2wt% Y_2O_3 to bioactive MgO–CaO–SiO_2–P_2O_5–CaF_2 glass leads to glass-ceramic samples that have enhanced hardness, fracture toughness and compressive strength compared to parent glass. However, Y_2O_3-modified glass-ceramic decreased the bioactivity of the original parent glass [43].

NiO doped bioactive glass-ceramics were prepared by melting and quenching. NiO concentration was varied between 0.4-1.65 mol% [44]. Increasing the NiO content, flexural strength (three-point bending) increased from 106MPa to 120MPa. Similarly, compressive strength increased from 112 MPa to 133MPa and Knoop microhardness values increased from 7.65 to 8.15 (GPa). The observed increase of mechanical properties is due to formation of Ni–O–Si bonds in the silicate network (glass phase structure) and crystallisation of sodium calcium silicate phases (ceramic phase structure). NiO doped bioactive glass-ceramics were confirmed to be bioactive and non-cytotoxic for rabbit osteoblast bone cells [44].

ZrO_2 doped AW bioactive glass-ceramics were obtained by multistep sintering AW and monoclinic ZrO_2 ($mZrO_2$) or 8wt% Y_2O_3 partially stabilized tetragonal ZrO_2 ($tZrO_2$) mixtures at temperatures between 700-1000 ^oC [45]. The amount of $mZrO_2$ or $tZrO_2$ in the $mZrO_2$-AW

or $tZrO_2$-AW glass-ceramic mixtures was varied between 2-8wt%. The main crystalline phases were $Ca_5(PO_4)_3F$ (fluorapatite) and β-CaSiO3(β-wollastonite). $mZrO_2$ slightly improved the fracture toughness of $mZrO_2$-AW glass-ceramics but decreased hardness and bending strength. $tZrO_2$ significantly increased the fracture toughness, bending strength and Vickers microhardness of $tZrO_2$-AW glass-ceramics [45]. The maximum values for bending strength and fracture toughness were achieved by $tZrO_2$-AW glass-ceramics containing 5wt% of $tZrO_2$ ($5tZrO_2$-AW glass-ceramic). Thus, by adding 5wt% of $tZrO_2$ the fracture toughness increased from 0.92 ± 0.02 MPa•$m^{1/2}$ (for pure AW glass-ceramic) to 1.67 ± 0.01 MPa•$m^{1/2}$ (for $5tZrO_2$-AW glass-ceramic), while bending strength increased from 37.17 ± 0.54 MPa (for pure AW glass-ceramic) to 46.41 ± 0.23 MPa (for $5tZrO_2$-AW glass-ceramic). Elastic modulus slightly increased from 19.2 ± 0.14 GPa for pure AW glass-ceramic to 21.6 ± 0.11 GPa for $5tZrO_2$-AW glass-ceramic, while microhardness increased from 114.19 ± 0.76 (GPa) for pure AW glass-ceramic to 145.44 ± 0.72 (GPa) for $5tZrO_2$-AW glass-ceramic. $5tZrO_2$-AW glass-ceramics are bioactive and showed no cytotoxicity for L-929 fibroblasts cells. The coefficient of thermal expansion of ZrO_2 doped AW bioactive glass-ceramics is close to that of titanium alloy (Ti6Al4V), so these glass-ceramics could be used as bioactive coatings for Ti_6Al_4V substrates [45].

4. Mechanical properties of "traditional" bioceramics: from almost-inert ceramics to calcium phosphates

Ceramics are usually hard and brittle materials, which possess elastic moduli within the range of human cortical bone. Bioinert ceramics like Al_2O_3 and ZrO_2 are highly durable and possess excellent mechanical strength, hence they are used as artificial femoral heads and acetabular cups [46]. Al_2O_3 has been widely used for manufacturing prosthetic bearings as it possesses high wear resistance, high strength and excellent corrosion resistance. High-purity Al_2O_3 (>99.5%) was the first bioceramic to be used clinically for load-bearing hip prostheses

and dental implants. Small amounts of MgO are added to Al_2O_3 to aid sintering and limit grain growth process.

Zirconia has replaced Al_2O_3 or has been combined to Al_2O_3 for many applications due to its higher toughness. Yttria-stabilised zirconia has been used as an alternative ceramic for femoral head and acetabular cup, as it possesses higher strength and fracture toughness than alumina [47, 48, 49, 50]. Despite their good biocompatibility, toughness and low friction, alumina and zirconia are not bioactive. This is the main reason why calcium phosphate bioceramics, exhibiting higher compositional and microstructural similarity with the mineral phase of bone, have been proposed to regenerate bone in osseous defects. This wide class of biomaterials has been comprehensively reviewed by Dorozhkin [51].

The mechanical strength of hydroxyapatite is particularly promising for bone substitution, also considering that it does not tend to drop down over time as this material is typically non-resorbable or very slowly resorbable, unless it is synthesized in the form of nano-sized particles [52].

Hsu and co-workers studied the mechanical properties of three different compositions of calcium phosphate bioceramics following immersion in Ringer's solution [53]. Table 2 presents the composition of the three samples with different ratios of α-TCP/β-TCP/HA.

Table 2 Calcium phosphate bioceramic composition (wt%) [53]

Sample Name	α-TCP	β-TCP	HA
COMP 1	2.31	21.73	75.96
COMP 2	20.81	41.98	37.21
COMP 3	0	96.72	3.28

The four-point bending strength of the three samples after 26 weeks immersion in Ringer's solution at pH7.2 and distilled water at pH4.0, is shown in Figure 1 [53].

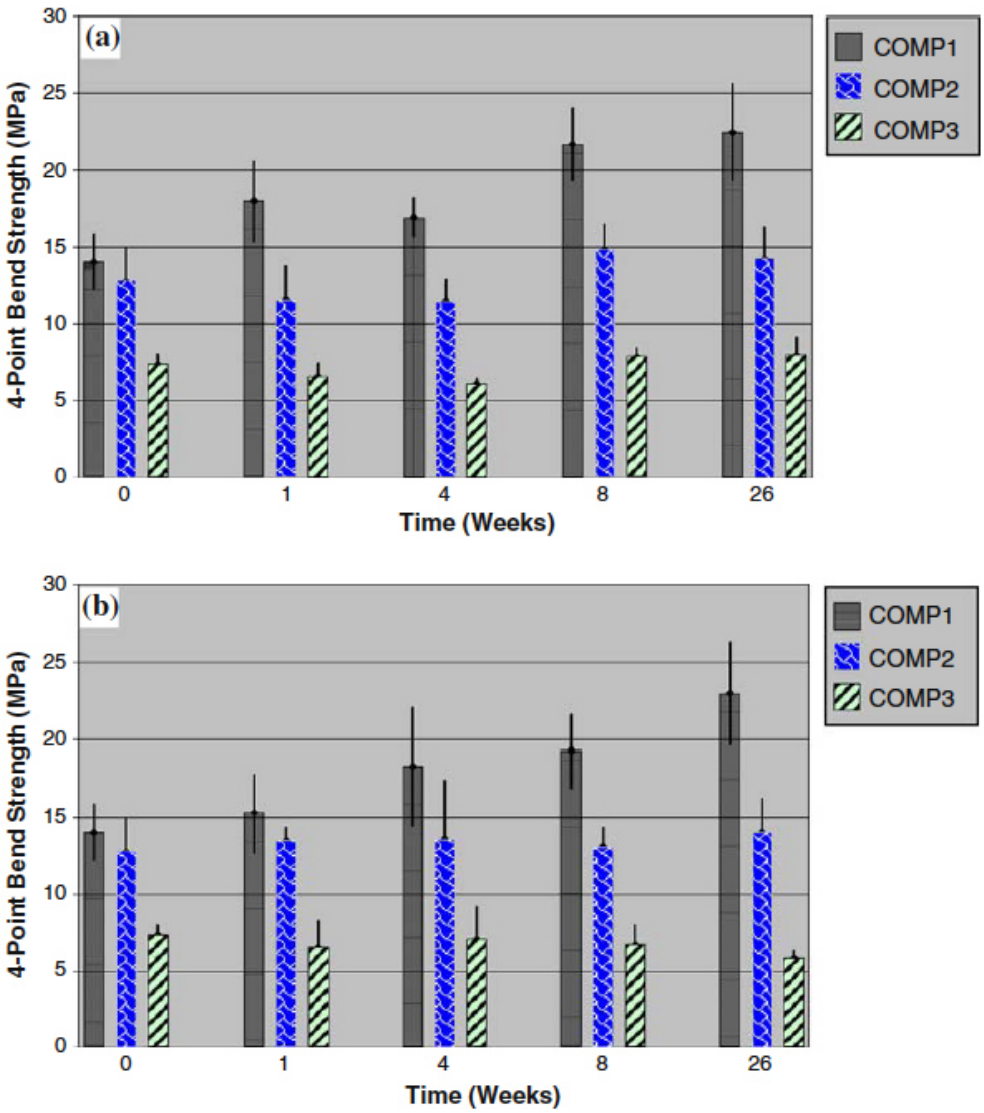

Figure 1 Four-point bending strength after immersion in (a) Ringer's solution at pH 7.2 and (b) distilled water at pH 4.0, for 26 weeks [53]

COMP1, having the highest HA content (75.96 wt%) has the highest four-point bending strength, whereas, COMP3 with the lowest HA content (3.28 wt%) has the lowest strength, irrespective of the solution type and immersion time. There is no statistical difference between the four-point bending strength in Ringer's solution and distilled water during the 26 weeks immersion time. Similar results were obtained for compressive strength for samples immersed in Ringer's solution or distilled water for 26 weeks. Compressive strength increases with the increase of HA content from 20MPa (COMP3) to 160MPa

(COMP1). A similar range of variation was achieved for compressive strength in both solutions (Ringer and distilled water) during 26 weeks immersion time [53].

Though hydroxyapatite is the most common osteoconductive material used for bone tissue engineering, it has lower fracture toughness and higher compressive modulus than human cortical bone (Table 1). These variations may lead to structural incompatibilities between implants and natural tissue and premature failures.

5. Mechanical properties of silicate bioceramics

Silicon (Si) is considered as the vital trace elements located at the active calcification sites in the bones inside the human body [54]. Si has been found to be directly involved in the bone mineralization during the bone growth process. Bone and extracellular matrix compounds contain almost 100 ppm and 200–550 ppm levels of silicon, respectively [55]. Looking at the importance of silicon inside the human body, various Si doped bioceramics have been widely researched [56, 57, 58]. Some particular compositions of calcium silicate ceramics possess unique bioactive properties and are found to enhance the in vitro osteogenic as well as angiogenic differentiation of the stem cells [59, 60, 61, 62]. To date, more than 20 calcium silicate bioceramics with a broad range of compositions have been fabricated during the past decade.

The preparation techniques significantly affect the mechanical properties of the calcium silicate bioceramics. Techniques like chemical precipitation, solid-reaction method, sol-gel method and hydrothermal method are used to synthesize the silicate bioceramics [58, 59, 60, 61]. Bioceramic monoliths can be fabricated using the pressureless sintering technique or spark plasma sintering (SPS).

Compared to the conventional phosphate-based bioceramics such as HA and TCP, calcium silicate bioceramics have extensive chemical compositions, which tailor their physicochemical properties, such as bioactive behaviour, mechanical strength and

degradation mechanism. Table 3 lists the main calcium silicate bioceramics with composition, mechanical properties, apatite mineralization and dissolution behaviour.

Table 3 Composition, mechanical properties, apatite mineralization and dissolution behaviour for the calcium silicate bioceramics [58, 61, 62, 63, 64, 65, 66, 67, 68, 69, 70, 71, 72]

Ceramic	Form	Composition	System	Bending strength (MPa)	Elastic modulus (GPa)	Compressive strength (MPa)	Fracture Toughness (MPa • $m^{1/2}$)	Apatite Mineralization	Dissolution behaviour
Wollastonite	Binary	$CaSiO_3$	Powder	294	46.5	60	2	Excellent	Rapid
Dicalcium silicate	Binary	Ca_2SiO_4	Ceramics	26-97	10-40		1.1-1.8	Excellent	Rapid
Tricalcium silicate	Binary	Ca_3SiO_5	Scaffolds Coatings	93.4	36.7		1.93	Excellent	Rapid
Magnesium silicate	Binary	$MgSiO_3$	Ceramics	32	8.5			Poor	Very slow
Dimagnesium silicate	Binary	Mg_2SiO_4	Powder	203			2.4	Poor	Very slow
Monticellite	Ternary	$CaMgSiO_4$	Scaffolds	159	51		1.63	Moderate	Slow
Merwinite	Ternary	$Ca_3MgSi_2O_8$		151	31		1.72	Good	Moderate
Diopside	Ternary	$CaMgSi_2O_6$	Spheres	300		0.2-1.36	3.50	Moderate	Slow
Akermanite	Ternary	$Ca_2MgSi_2O_7$	Powder			0.53-1.13	0.63-1.72	Good	Moderate
Bredigite	Ternary	$Ca_7MgSi_4O_{16}$	Ceramics	156	43	0.233	1.57	Excellent	Rapid

Hardystonite	Ternary	$(Sr,Ca)SiO_3$ $Zn_{(x)}CaSiO(3+x)$ $Ca_2ZnSi_2O_7$	Ceramics Ceramics Powder	136	37		1.37	Poor	Very slow
Strontium hardystonite	Ternary	$Sr_2ZnSi_2O_7$ $CaNa_2SiO_4$ $Ca_2Na_2Si_3O_9$	Ceramics Ceramics Ceramics					Poor	Very slow
Baghdadite	Ternary	$Ca_3ZrSi_2O_9$	Ceramics Spheres					Moderate	Slow
Sphene	Ternary	$CaTiSiO_5$	Ceramics Coatings					Poor	Very slow
Silicocarnotite	Ternary	$Ca_5P_2SiO_{12}$	Powder	65	80			Good	Moderate
Nagelschmidtite	Ternary	$Ca_7Si_2P_2O_{16}$	Ceramics					Excellent	Rapid
Strontium silicate	Binary	$SrSiO_3$	Powder					Good	Moderate
Zinc silicate	Binary	Zn_2SiO_4	Ceramics	91	37.5			Poor	Very slow
Zinc silicate	Quaternary	$(Sr,Ca)_2ZnSi_2O_7$	Scaffolds						

HA possesses maximum fracture toughness and bending strength of 1.2 MPa $m^{1/2}$ and 120 MPa, respectively. As evident from table 3, the fracture toughness for many silicate bioceramic like diopside, wollastonite, dicalcium silicate, monticellite, akermanite, bredigite and hardystonite etc. is generally higher than that of HA [61]. The bending strength and elastic modulus for most of the silicate ceramic monoliths is comparable to the human cortical bone (table 1). SPS-sintered calcium silicate ceramics, such as dicalcium silicate and wollastonite, have appreciably enhanced mechanical properties, as compared to the conventional pressureless-sintered calcium silicate ceramics [**73**].

Calcium silicate bioceramics also possess the distinct ability of apatite mineralization as shown in table 3. The chemical compositions and dissolution of bioceramics describes the apatite mineralization ability. Wollastonite, tricalcium silicate, dicalcium silicate, nagelschmidtite and bredigite ceramics exhibit the best apatite mineralization capacities along-with rapid dissolutions in SBF. Merwinite, akermanite, silicocarnotite and strontium silicate display good apatite mineralization and reasonable dissolutions. No observable apatite mineralization could be seen for the hardystonite bioceramics and their dissolution is also quite low. Usually, improved apatite mineralization could be observed for the calcium silicate bioceramics with high Ca contents. When metal ions like Mg, Zn and Zr are incorporated into the calcium silicate ceramics, then the apatite mineralization ability is noticeably decreased. As evident from table 3, the bioceramics with fast dissolutions yield enhanced apatite mineralization, indicating that dissolution rate linearly affects the mineralization capability.

Despite having higher mechanical properties than calcium phosphate ceramics, forsterite Mg_2SiO_4 (M_2S) ceramics have lower mechanical strength than cortical bone and cannot be used for load-bearing applications. Despite M_2S having good biocompatibility it has low degradation rate and poor apatite-formation ability [74]. Hence, research was focused

on developing nanostructured materials based on bioactive forsterite ceramics. Webster and co-workers designed the first nanosize ceramics with improved osteointegration properties [75]. Kim and co-workers obtained improved biocompatibility, osteoblast adhesion and proliferation for the nanostructured materials due to a high fraction of grain boundaries [76]. Nanosized forsterite exhibited better apatite formation ability when compared to the forsterite microparticles. Kharaziha and Fathi [77] prepared dense forsterite ceramic discs using a two steps sintering of sol-gel derived powder [78], to avoid grain growth during the conventional sintering process. Pressed discs (sol-gel derived green bodies) were heated up to 600 °C for 60 min, followed by heating to temperatures in the range 900–1300 °C (T1) for 6 min (step 1). After heating, the samples were cooled down to 750 °C or 850 °C for 2h, 5h or 15h (step 2) [77]. The dense discs obtained after this two-step sintering process had fracture toughness in the range 1.0–4.3 MPa•$m^{1/2}$ and Vickers hardness HV of 475–1000 (MPa). These values are higher than those of hydroxyapatite (0.8–1.2MPa•$m^{1/2}$and 90–140 (GPa)), reported in Table 1. Fracture toughness and Vickers hardness of forsterite samples as a function of sintering temperature T1 are presented in Figure 2. These samples also showed good biocompatibility for G292 osteoblast cells [77].

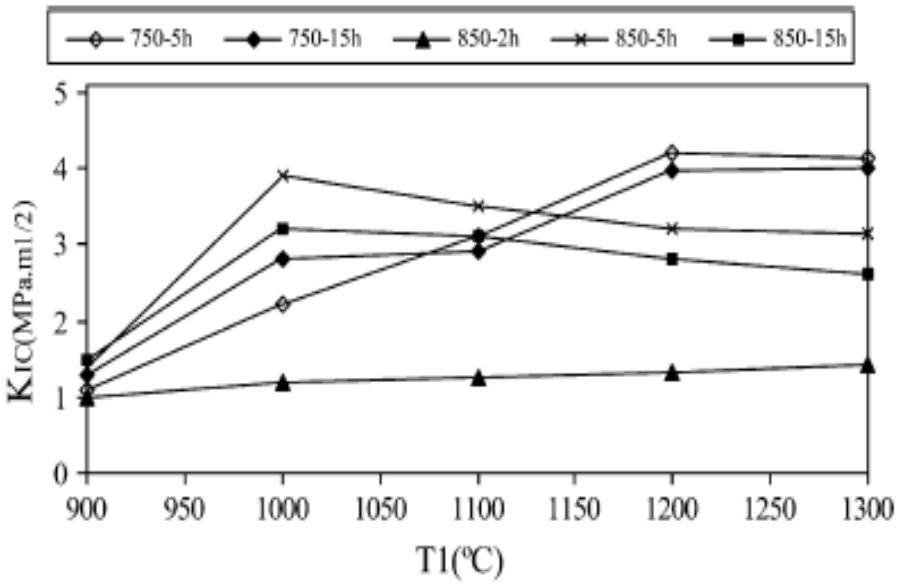

a)

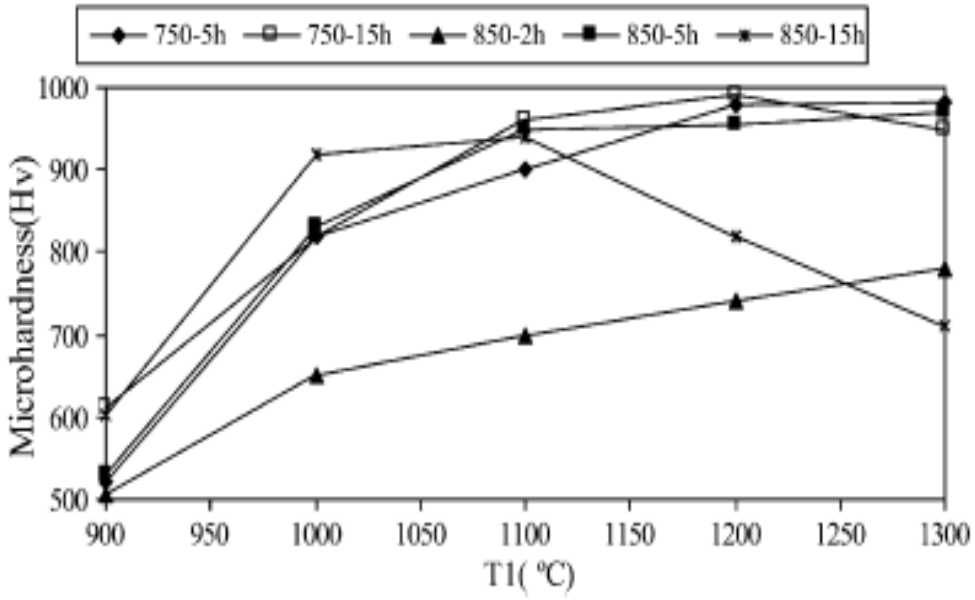

b)

Figure 2 a) Fracture toughness (MPa • $m^{1/2}$) and b) Vickers hardness (MPa) for the forsterite samples as function of sintering temperature of the first step (T1) [77]

The two-step sintering method used by Kharaziha and Fathi [77] is very different from conventional sintering methods. In a typical conventional sintering method, green body compacts are heated in one step at a high temperature and held at that temperature until a higher densification level is achieved. The grain size increases continuously as density increases, leading to lower values of fracture toughness. In the two-step sintering method green body compacts are heated to a high temperature and held for a short time (6 minutes) to reduce the pore sizes to less than 1μm, followed by cooling to a lower temperature for a longer time (hours), in order to complete the sintering process. Samples heat treated at 1200 °C (T1) and 750 °C (T2) for 5h or 15h showed the highest values of fracture toughness and Vickers hardness (Figure 2). Increasing the sintering time of step 2 from 2h to 5h (T1 = 1200 °C, T2 = 750 °C), the density of the resulted samples increased from 80% (after 2h) to approximately 99% (after 5h). Thus, the two-step sintering method (T1 = 1200 °C/6min, T2 = 750 °C/5h) yields the optimization of mechanical strength and grain size, as highly dense forsterite ceramics (98.6 ± 0.22 %) with small crystallite size (30–45nm), high fracture

toughness of 4.3 ± 0.2 MPa•$m^{1/2}$ and high hardness values 1100 ± 25 (MPa) have been obtained [77].

Siyu Ni and co-workers [79] synthesised highly dense forsterite from coarse grain forsterite powder with relative density of 92.9% by uniaxial pressing at 10MPa and then cold isostatic pressing at 200 MPa. The samples were sintered at 1450 °C for 8 h and the maximum fracture toughness value was 2.4 MPa•$m^{1/2}$.

$CaSiO_3$ (CS) ceramics have relatively rapid apatite formation and high growth rate of the apatite layer in SBF [74]. However, they also exhibited a relatively fast degradation rate and poor mechanical properties. *In vivo* experiments showed that the CS coatings have good osteoconduction [74]. Combination between CS and forsterite M_2S leads to ceramics with improved mechanical properties and apatite formation ability. By varying the initial CS/M_2S ratio, bending strength and compressive modulus increased compared to pure CS ceramics. Varying the M_2S percent from 0 to 70%, the bending strength increased from 33MPa to 185MPa, while compressive modulus increased from 16GPa to 30GPa [74]. Pure CS has a relatively high dissolution rate while M_2S has a lower dissolution rate. Increasing the amount of CS also increases the solubility of CS/M_2S ceramics [74].

6. Mechanical properties of bioactive hybrids

The bioactive glass composition can be modified with organic polymers to provide mechanical properties similar to natural bone. Bioactive glass/polymer hybrids were found to more closely match the low elastic modulus of bone while exhibiting increased toughness, strength and fatigue resistance [30, 74, 79].

Organic-inorganic hybrid materials are mixed at the molecular level with or without the aid of coupling agents and form a chemical bond between the organic and inorganic phase. A coupling agent can functionalize the polymer to form a covalent bond with the inorganic phase. The inorganic phase is a sol-gel derived silica glass. Due to the covalent bonding

between the organic and inorganic phases, their mechanical properties are higher than the individual components.

One of the polymers used as a precursor for sol-gel derived organic-inorganic hybrid biomaterials is poly(dimethyl siloxane) (PDMS, $Si(OC_2H_6)_n$). PDMS-derived hybrids form a covalent bond between the silica network and PDMS. However, these hybrids are not bioactive unless Ca^{2+} ions are incorporated in the network [80]. Other polymers used to prepare organic-inorganic hybrids include polyethylene glycol, gelatin, poly(ε-caprolactone) (PCL) [81]. Silica based sol-gel hybrids that employ self-hardening copolymers of methyl methacrylate (MMA) and 3-(trimethoxysilyl) propyl methacrylate (TMSPMA) have been reported [82].

PCL/silica hybrids were obtained via sol-gel process, using 3-isocyanatopropyl triethoxysilane (IPTS) as a coupling agent. The stability of the hybrid structure increases by cross-linking, which is controlled by the molecular weight of the polymer. Using lower molecular weight PCL leads to increased cross-linking and faster apatite formation. Decreasing the amount of PCL in the hybrid, increased the apatite forming rate but the material showed brittle fracture behavior [83].

PCL/borosilicate glass hybrid biomaterials containing 50wt% trimethoxysilane-functionalised polycaprolactone (PCL) and 50wt% boro-phospho-silicate (B_2O_3-P_2O_5-SiO_2) glass (BPSG) exhibited compressive strength, modulus and toughness values of 32.2±3.5 MPa, 573±85 MPa and 1.54±0.03 MPa, respectively. These were almost double the values observed from composites of similar composition, obtained using pure PCL (non-functionalised PCL) [81].

Poly(amido amine) / 70S30C bioactive glass inorganic-organic hybrids were developed using 3-glycidoxypropyltrimethoxysilane (GPTMS) as coupling agent. These hybrids are

bioactive, non cytotoxic for human gingival fibroblast cell lines and showed antibacterial properties against *Staphylococcus aureus* [84].

When bioactive glasses containing silica and titania are intimately combined with flexible organic components at the nanoscale, bioactive hybrid materials with low elastic moduli can be obtained [85, 86, 87, 88, 89]. Functional groups as Si-OH and Ti-OH can promote nucleation and growth of apatite crystals in SBF, especially when Ca^{2+} ions are released from the surface of the biomaterial [90]. The inorganic component of these hybrids is usually derived from tetraethoxy silane (or tetraethyl orthosilicate, TEOS) or tetra isopropyl titanate (TiPT) whereas the organic component is derived from PDMS or polytetramethylene oxide PTMO terminated with 3-isocyanatopropyltriethoxysilane (IPTS) [85]. These hybrids possess elastic moduli similar to human cancellous bone but they do not exhibit apatite-forming behaviour unless CaO is present in the inorganic precursors. Therefore, calcium salts such as $CaCl_2$ or $Ca(NO_3)_2$ are incorporated into these hybrids to improve bioactivity, even if this may involve a reduction in mechanical strength [85].

Tsuru at al [91] and Yabuta et al [92] fabricated bioactive organic-inorganic hybrids using PDMS, TEOS and $Ca(NO3)_2$ through a sol-gel process. By incorporation of highly reactive Ti alkoxides (TiPT) Chen at al [86] obtained hybrids with higher mechanical strength [93]. A similar approach was suggested by Aburatani et al [94] who modified the synthesis method proposed by Tsuru [91] by the addition of colloidal silica, to increase the mechanical properties. Increasing the content of colloidal silica resulted in increased compressive strength of these hybrids [94].

Miyazaki and co-workers [90] synthesized bioactive organic-inorganic hybrids using hydroxyl ethyl methacrylate (HEMA), tetra isopropyl titanate (TiPT) and $CaCl_2$. HEMA provides high hydrophilicity and biocompatibility, while TiPT provides Ti-OH groups that promote apatite nucleation and crystallisation. Young's modulus varied between 0.04-

6.4MPa, being similar to human articular cartilage (1-10MPa). Increasing the TiPT content, the tensile strength and Young's modulus increased. However, tensile strength values varied between 0.4-7MPa, being lower than the values for human articular cartilage (10-40MPa) [90].

One of the polymers that has been developed for soft tissue regeneration is poly(glycerol sebacate) (PGS) elastomer. However, PGS has low bioactivity, hydrophilicity and tensile strength (0.3 to1.5 MPa), limiting its applications for bone, cartilage or tendon regeneration [95]. Zhao and co-workers developed PGS-silica-based bioactive glass hybrid elastomers (PGS-SC) by a direct hybridization method. The silica-based bioactive glass is a $CaO\text{-}SiO_2$ glass obtained by a sol-gel process, using TEOS and $CaCl_2$ as main reagents. The PGS polymer solution was dissolved in ethanol and then mixed with the glass sol. The resulted PGS-SC hybrid showed enhanced hydrophilicity and degradation compared with pure PGS [95]. The tensile strength increased notably from 1.13 ± 0.1 MPa for pure PGS to 4 ± 0.84 MPa for PGS-SC, while elastic modulus increased from 1.75 ± 0.15 MPa (pure PGS) to 34.52 ± 4.73 MPa (PGS-SC). PGS-SC is bioactive after immersion in SBF and non cytotoxic for MC3T3 osteoblasts [95].

3D-printable hybrids with "bouncy" elasticity and self-healing ability were also recently proposed by Tallia et al. [96] for osteochondral applications.

7. Mechanical properties of bioactive glass-ceramic scaffolds

Bioactive glasses can also be processed to obtain three-dimensional (3D) scaffolds that should exhibit a highly-interconnected macroporous structure (pore size above 100 μm) to promote bone integration [97]. Furthermore, porosity promotes vascular ingrowth, resorption, bioactivity and osteoblast differentiation [98]. Porous scaffolds are commonly produced by high-temperature sintering of glass particles following the shaping/moulding stage [99].

However, the famous 45S5 glass composition has poor sinterability and, thus, scaffolds made of this glass cannot be produced without partial crystallization. Specifically, 45S5 Bioglass forms crystalline $Na_2CaSi_2O_6$ when treated above 550-600 °C [100], which is very close to its glass transition temperature; hence, crystallization is almost unavoidable during sintering [101]. The presence of crystalline phases can significantly slow the formation rate of nano-crystalline hydroxyapatite on the material surface; however, it was reported that 45S5 composition still maintains a weak bioactivity even after achieving 100% of crystallinity [102, 103].

The first 4S55 Bioglass-derived glass-ceramic scaffolds were produced in 2006 by sponge replication but the poor glass sinterability led to porous structures with hollow struts and, thus, compressive strength unacceptable for bone repair (<0.4 MPa vs. 2-12 MPa) [104].

Since then, different strategies have been proposed to improve the mechanical strength of 45S5-based scaffolds, including mixing the 4S55 Bioglass with a small amount of other glass, which acts as a sintering aid, and/or increasing the sintering temperature. Xu and co-workers [105] fabricated glass-ceramic scaffolds by sintering mixtures of 4S55 bioglass and a sol–gel derived calcium borosilicate glass CBS (19.5 B_2O_3–48.2CaO–30.2SiO_2–2.1P_2O_5 wt%). 45S5/CBS porous scaffolds were obtained by mixing 45S5/CBS powder mixtures (with a CBS content of 0-20wt%) with paraffin particles (280-400μm) using a mass ratio of 65:35 (45S5/CBS:paraffin). The resulting powder mixtures were pressed into cylindrical shape moulds using a uniaxial press at 4MPa. The samples were then sintered at 800–1100 °C for 2h [105]. Increasing the sintering temperature from 800 °C to 1000 °C the compressive strength of 4S55/CBS10 scaffolds containing 10wt% CBS increased from 3MPa to 12MPa, while the porosity decreased from 76% to 64%. Thus, the boron-rich CBS glass can significantly reinforce the 45S5 bioglass when 4S55/CBS scaffolds are sintered at 850–900 °C [105]. CBS glass having a melting temperature of ~960 °C [106, 107] and a

lower sintering temperature, assists bonding between 45S5 and CBS particles by viscous flow in the porous scaffolds. Above a sintering temperature of 800°C, 4S55 starts to crystallise forming mainly $Na_2Ca_2Si_3O_9$ crystalline phase, while CBS glass starts to soften. At temperatures of 850–900°C, the intergranular CBS liquid-phase covers the 45S5 particles, enhancing the strength of the scaffolds. Thus, liquid phase sintering of 45S5/CBS10 mixtures at low temperatures (850–900°C) produced scaffolds with a compressive strength of 7-9MPa and a porosity of 70-74%, similar to the values of the human trabecular bone. 10wt% CBS reinforced 45S5 porous scaffolds (4S55/CBS10) sintered at 850–900 °C showed good bioactivity and biodegradability. Immersion in Tris buffer solution for 14 days leads to a slight decrease (1-2MPa) of compression strength for 45S5/CBS10 scaffolds sintered between 800 °C and 1000 °C [105]. However, the scaffolds maintained their stability and can provide a temporary mechanical support for bone ingrowth.

45S5 Bioglass-derived and CEL2-derived glass-ceramic scaffolds were fabricated using the sponge replication technique, pushing to the limit the sintering temperature in an attempt to achieve good densification of scaffold struts and high mechanical properties while maintaining a total pore content comparable to that of human cancellous bone (>50 vol.%). CEL2 is a silicate glass containing MgO and K_2O in addition to the 45S5 composition. Despite their high porosity (~70 %vol.), compressive strength of ~2.5 MPa and ~4.5MPa, comparable to that of cancellous bone, were obtained for Bioglass-derived and CEL2-derived glass-ceramic scaffolds, respectively. The difference in mechanical strength was attributed to the different sintering behaviour of the two starting glasses [108].

Apatite-mullite (AM) and apatite-wollastonite (AW) glass-ceramic scaffolds were fabricated using an indirect selective laser sintering (SLS) method by Dalgarno and co-workers [109]. Powders with particles size in the range 45-90μm or powder mixtures with different fraction between 45-90μm and 0-45μm particles size have been used for SLS. AW

green bodies produced by SLS were sintered using a two-step sintering process: 779℃ for 1h (step 1) to achieve optimal nucleation and 1150℃ for 1h (step 2) for crystal growth. AM green bodies produced by SLS were sintered using a one-step sintering process. AM green bodies were placed into a furnace at 1200 °C for 1h, followed by cooling. After sintering the AM and AW scaffolds have a porosity of 40-50% and open porous structures required for bone ingrowth and vascularisation [109]. The flexural strength (three-point bending) of AM and AW scaffolds was 7-38MPa (depending on the initial fraction of fine (0-45μm) and coarse (45-90μm) particles size), being similar to the values reported for trabecular bone (10-20MPa, Table 1). AM scaffolds with 100% coarse 45-90μm powder had the lowest flexural strength (7MPa). The flexural strength of these AM scaffolds increased to 12-20MPa by mixing coarse and fine powders to produce green bodies or by infiltration of sintered AM scaffolds with a phosphate glass at 1200 °C for 1h (flexural strength 14MPa). AW scaffolds with 100% coarse 45-90μm powder had the highest flexural strength (32-39MPa) [109]. This increase in strength can be explained by the corresponding reduction of porosity. The infiltration process reduced the scaffolds porosity significantly, while the use of powder mixtures with different fraction of fine and coarse powder sizes preserves the porosity around 40% [109].

Furthermore, silicate scaffolds have been prepared using porogen method, polyurethane foam templating method and 3D plotting technique. Porogen method yields good mechanical strength of the scaffolds, but pores were not interconnected or uniform [110]. Conversely, the template method provides enhanced interconnectivity along with large pore size; however, the scaffolds prepared were not mechanically strong. The 3D plotting technique offers the advantage of precise control of the scaffold structure and mechanical strength, attributed to layer by layer plotting under suitable mild conditions [111, 112].

Porogen method usually endows the scaffolds with high compressive strength attributed to their low porosity and interconnectivity. Wollastonite scaffolds synthesized using porogen method had a compressive strength of 60 MPa. However, when wollastonite scaffolds were fabricated using polyurethane foam templating method and 3D plotting technique, the compressive strength was 0.4 MPa and 3.6 MPa, respectively, these values being much lower than the ones obtained from the porogen technique. Figure 3 depicts the stress-strain curve for 3D-printed $CaSiO_3$ scaffolds. Remarkably, these scaffolds partially retain their shape after the compressive test (figure 3c) [113].

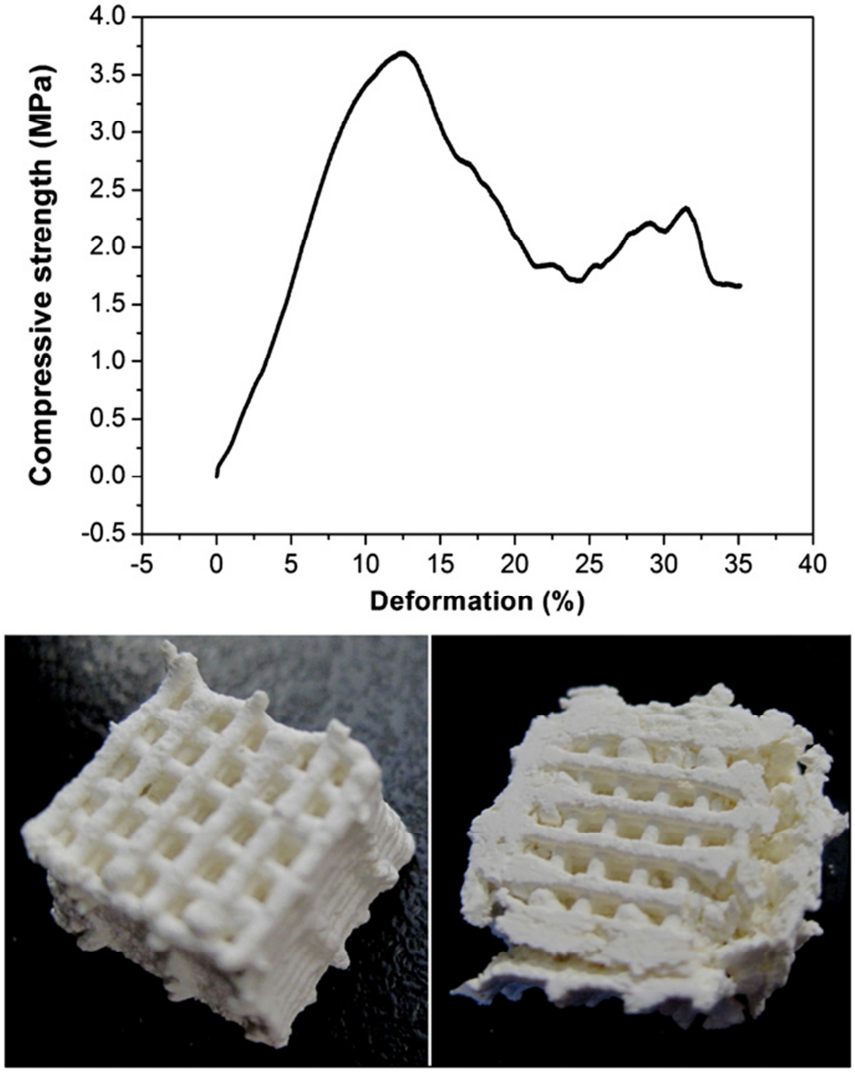

Figure 3 a) Compressive strength for the $CaSiO_3$ scaffolds; scaffolds before (b) and after (c) compression testing [113].

8. Mechanical properties of bioactive glass scaffolds

The development of glass scaffolds with low tendency to devitrification upon thermal treatment is often preferred when bone repair is the major goal, since the apatite-forming ability and bone-bonding of these materials is dictated by the ion-exchange reactions between amorphous phase and biological fluids [114]. A typical example is represented by the glass composition 13-93, which has received approval for clinical use in Europe and USA [115]. On the other hand, glass-ceramic scaffolds embedding crystalline phases in a residual glassy matrix often exhibit higher mechanical properties than their glass counterparts; however, the use of additive manufacturing approaches has recently allowed strong glass scaffolds with highly-promising mechanical properties for bone repair to be obtained.

In this regard, 45S5-derived and 13-93 bioactive glass scaffolds with mechanical properties similar to those of cortical bone have been fabricated using 3D printing technique (robocasting or direct ink printing) [116]. This process enables the formation of scaffolds with grid-like structures and straight channels with open porosities in x, y, and z directions. The robocasting process involves dispersing glass powder into a suitable binder, to create an ink. The printed green body is then sintered into strong glass scaffolds while the binder burns out [116]. In order to be used for robocasting, the ink should have appropriate shear thinning rheology to flow easily through a fine diameter nozzle under force. After extrusion the ink should be mechanically stable and not deform, and it should dry without producing cracks in the extruded filaments. Mechanical stability of the green body depends on the physical and chemical properties of the ink, particle size of the glass, and pore size distribution [116]. The most common polymeric binders that have been used to produce bioactive glass scaffolds by robocasting are Pluronic F-127, ethyl cellulose/polyethylene glycol, and carboxymethyl cellulose [116].

Liu and co-workers [117] also prepared grid-like porous scaffolds of 13–93 silicate glass (53SiO_2, 6Na_2O, 12K_2O, 5MgO, 20CaO, 4P_2O_5 wt.%) using robocasting techniques (Figure 4a). After printing, the samples were dried for one day in air at room temperature, heated to 600 °C in O_2 to burn out the processing additives, and sintered in air for 1h at 700 °C. The resultant scaffolds have a grid-like microstructure with pore width of 300±10 μm in the deposition plane (xy plane) and pore height of 150±10 μm in the direction of deposition (z axis) [117]. The flexural strength and flexural modulus values were 11±3MPa and 13±2GPa, respectively, being close to the lower end of trabecular bone values [117]. The compressive strength and compressive modulus were 86±9MPa and 13±2GPa, respectively, being close to the cortical bone values (Table 1).

The Weibull plots of compressive strength (Figure 4b) and flexural strength (Figure 4c) are almost linear (R=0.92-0.93) except at low and high stress values [117].

(a) 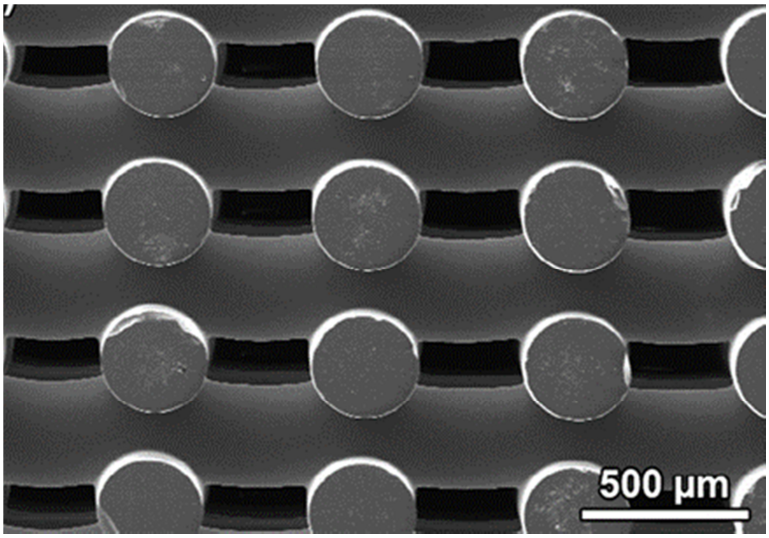

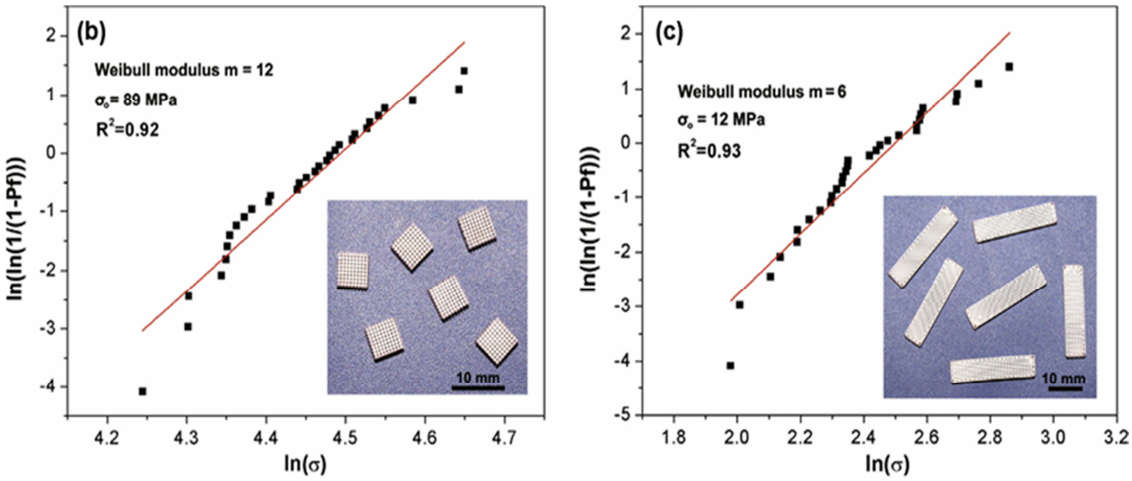

Figure 4 a) SEM of 13-93 scaffolds prepared by robocasting method, (b) Weibull plot of compressive strength and (c) Weibull plot of flexural strength for 13-93 scaffolds (adapted from [117])

The 13–93 scaffolds were tested under compressive cyclic stress between 1–30 MPa in air at room temperature and in phosphate buffered saline (PBS) at 37 °C using a frequency of 5Hz. All six samples tested under a cyclic stress of 1–10 MPa survived, showing that these samples had a fatigue life greater than 10^6 cycles. Increasing the stress amplitude to 30MPa the mean fatigue life decreased, but the difference was not statistically significant. For PBS fatigue testing, five out of six samples survived 10^6 cycles limit when a cyclic stress of 1–10 MPa was used. Increasing the stress amplitude to 30MPa the mean fatigue life decreased significantly [117].

Degradation of the compressive strength and compressive modulus of the 13–93 scaffolds was evaluated *in vitro* using a simulated body fluid (SBF) at 37°C. Degradation tests *in vivo* were analysed using scaffolds after subcutaneous implantation in different sites in the dorsum of rats for up to 3 months [117]. Both *in vitro* and *in vivo* studies showed a notable decrease of compressive strength and compressive modulus values within 2 weeks. However, after 2 weeks the mechanical properties changed more slowly for both *in vitro* and *in vivo* tests (Figure 5) [117].

The decrease of compressive strength and compressive modulus values *in vivo* was larger than that *in vitro* [117]. The compressive strength decreased from 86 ± 9 MPa to 58 ± 5 MPa after 2 weeks in SBF, and to 35 ± 4 MPa after the same time *in vivo* (Figure 5a). After 12 weeks of immersion in SBF the compressive strength of the scaffolds decreased to 52 ± 10 MPa, while the compressive strength of *in vivo* implantation was 16 ± 4 MPa after a similar time (Figure 5a) [117]. The compressive modulus decreased from 13 ± 2 GPa to 11 ± 1 GPa after 2 weeks in SBF, and to 6 ± 2 GPa after the same time *in vivo* (Figure 5b). After 12 weeks of immersion in SBF the compressive modulus of the scaffolds was 9 ± 2 GPa, while the compressive modulus after the same time of *in vivo* implantation decreased to 2 ± 1 GPa (Figure 5b) [117]. This decrease in mechanical properties is related to the formation of a porous hydroxyapatite layer and partial dissolution of the glass filaments [117].

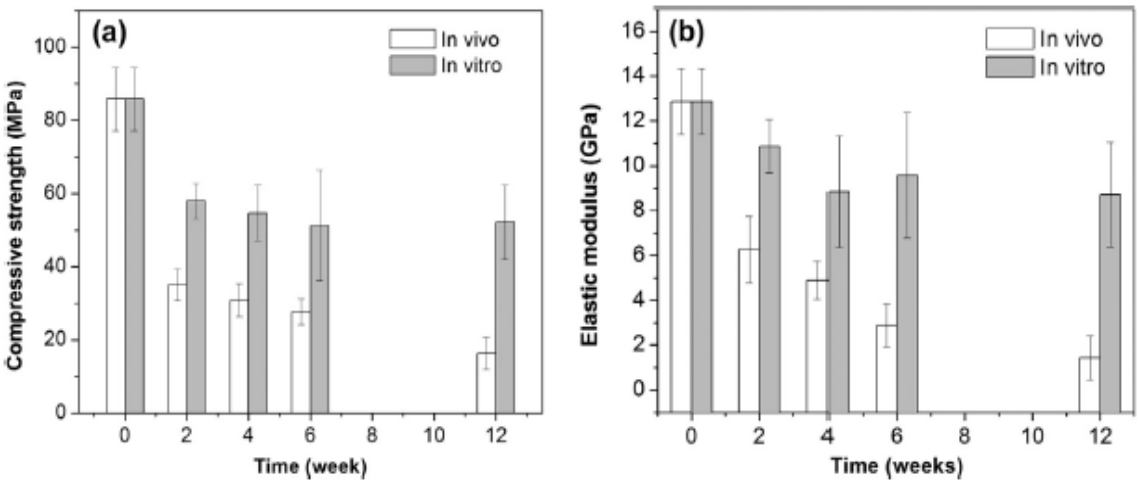

Figure 5 (a) Compressive strength and (b) compressive modulus for 13-93 scaffolds after immersion of the scaffolds in SBF at 37 °C (*in vitro*) and after subcutaneous implantation in rats for 12weeks (*in vivo*) [117].

Interestingly, the scaffolds implanted *in vivo* showed an increase in compressive strain values with the implantation time; instead of fracturing, they maintained their integrity. However, the fracture toughness of 13–93 scaffolds prepared by robocasting was 0.48±0.04 $MPa•m^{1/2}$, which is much lower than that of the human cortical bone (2–12 $MPa•m^{1/2}$) [117].

Kolan et al [118, 119] fabricated porous 13-93 bioactive glass scaffolds by indirect selective laser sintering (SLS) using stearic acid as a polymeric binder (Figure 6). They investigated the effect of particle size distribution, binder content, SLS processing parameters (laser power, beam speed and scan spacing) and sintering conditions (heating rate and temperature) on the mechanical properties of these scaffolds. Increasing the laser power and scan speed produced scaffolds with higher mechanical properties. The heating rate during sintering significantly affects the mechanical properties of the sintered scaffolds [119]. After optimization of all process parameters for 'green body' and sintered constructs, the compressive strengths of the sintered scaffolds varied from 41MPa for scaffolds with ~50% porosity to 157 MPa for dense scaffolds. After immersion in the SBF for 6weeks, the compressive strength of the porous scaffolds decreased but was in the range of human trabecular bone [119].

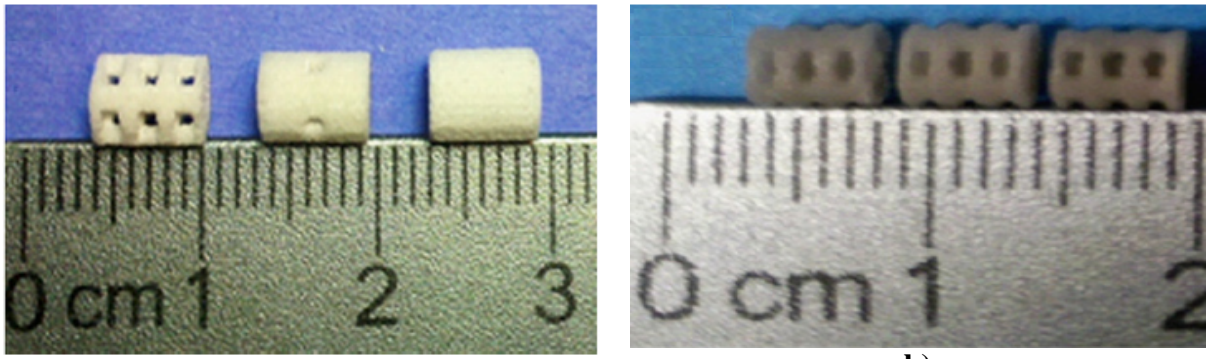

a) **b)**

Figure 6 Digital images of a) porous, hollow and solid 'green bodies' and b) sintered porous 13-93 glass scaffolds (adapted from [119])

For the purpose of comparison, it is instructive to mention the work reported by Fu and co-workers [120] who synthesized 13–93 porous glass scaffolds using a polyurethane foam replication method. The stress strain curve for a 13–93 glass scaffold sample is presented in Figure 7. The valleys and peaks in this diagram correspond to the progressive breaking down of the scaffold structure [120].

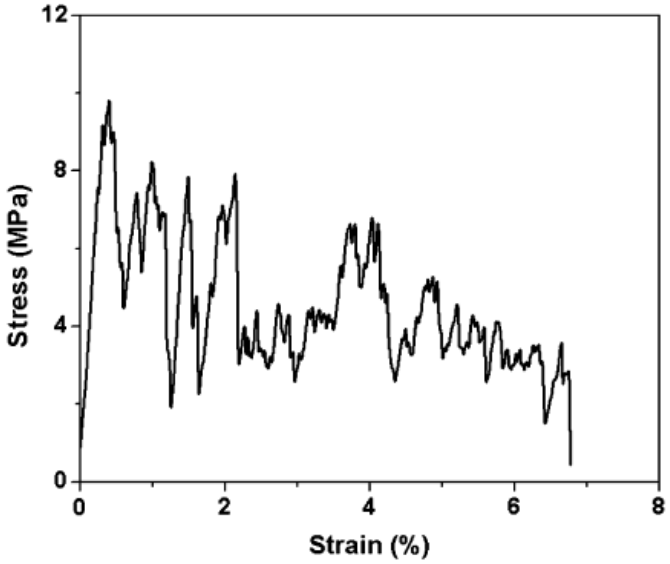

Figure 7 Stress strain curve for 13-93 glass scaffolds under compression [120]

During the initial compression, the glass showed elastic behaviour, followed by a decrease in stress attributed to the fracture of scaffolds' struts [120]. Eight samples were tested in compression (porosity 85 ± 2%). The average compressive modulus calculated from the initial linear region of the stress–stain curve was 3.0 ± 0.5 GPa, while the average compressive strength determined as the highest stress on the stress–strain curve was 11 ± 1 MPa (values similar to the compressive strength of human trabecular bone (Table 1) [120]. The measured compressive strength of the 13–93 glass scaffolds was higher than the values reported for hydroxyapatite scaffolds with similar porosity and polymer-ceramic composites prepared by the thermally induced phase separation (TIPS) method [120]. Glass–ceramic scaffolds with a porosity of 89–92%, obtained from 45S5 bioactive glass have a compressive strength of 0.3–0.4MPa. Hydroxyapatite scaffolds with a porosity of 86% had compressive strengths of 0.01–0.2 MPa, while those with porosity of 70–77% had higher values of compressive strength (0.6–5.0MPa) [120]. Hydroxyapatite scaffolds coated with apatite-wollastonite glass-ceramic and having a porosity of 93%, resulted in a compressive strength

of approximately 1MPa. Hydroxyapatite scaffolds prepared by gas foaming techniques and rapid prototyping had compressive strengths of 17MPa (73% porosity) and 30 MPa (35% porosity) respectively [120].

Mechanically-strong grid-like robocast scaffolds were also obtained by using 47.5B glass (47.5SiO_2-10Na_2O-10K_2O-10MgO-20CaO-2.5P_2O_5 mol.%) that was not prone to devitrification upon sintering [121]. The compressive strength (around 10 MPa for as-produced scaffolds) progressively decreased during immersion in simulated body fluids (3.3 MPa after 1 month) but it still remained comparable to that of human spongy bone. Thus, 47.5B glass has been considered acceptable for bone repair applications [122].

In general, it is apparent that additive manufacturing techniques exhibit higher versatility for processing bioactive glasses compared to "traditional" methods, showing great promise for the fabrication of hierarchical scaffolds based on mesoporous bioactive glasses (MBGs). Over the last decade, MBGs have been proposed as smart platforms for the controlled release of drugs, growth factors and therapeutic ions [123, 124] due to their controlled solubility in aqueous environment and the presence of an ordered texture of nanopores. The nanopore size can be finely controlled by varying some key parameters (e.g. pH, temperature) during the sol-gel process applied for their synthesis [125]. However, the size of mesopores (2-50 nm) [126] is several orders of magnitude smaller than bone cells (10-200 μm); this precludes cells from entering the pores and, hence, MBGs should be somehow processed by macro/meso-co-templating strategies to acquire multiscale porosity allowing bone cell penetration, attachment and proliferation.

Scaffold processing methods should indeed preserve the original mesoporosity of MBGs, which is exploited for encapsulating and releasing therapeutic biomolecules. Initially, hierarchical MBG scaffolds were produced by dipping a polyurethane foam into the sol, but dramatically brittle structures were obtained (compressive strength in the range of 50 to 250

kPa) [127]. An exceptional improvement is obtained when MBGs are processed by additive manufacturing strategies: Wu et al. [128] used 3D printing to fabricate SiO_2-CaO-P_2O_5 MBG hierarchical scaffolds with compressive strength of 16 MPa, along with excellent apatite-forming ability and sustained drug release. MBG scaffolds produced by 3D printing were also shown to retain good mechanical strength (7 MPa) after being soaked in simulated body fluids to mimic their evolution upon contact with body environment [129].

9. Mechanical properties of bioactive composite scaffolds

Composite materials consist of two or more distinct phases/constituents that are combined in order to produce a different material with tailored chemical, physical, mechanical and biological properties [130]. Composites offer the advantage of better mechanical and bioactive properties and hence have been an intense topic of research. Polymer matrix composites can be designed to combine mechanical properties of bioactive glasses, ceramics or glass-ceramics with the flexibility of polymers. Bone is a composite material, composed of carbonated apatite (65 dry wt%) that provides stiffness and structural reinforcement, and collagen (35 dry wt%) that provides flexibility and toughness [131]. Development of polymer-ceramic composites that mimic bone structure should lead to higher toughness for the composites compared to the pure ceramics.

The mechanical properties of bioactive ceramics and glasses, especially when fabricated in a porous form (scaffold) and therefore more susceptible to catastrophic failure, can be improved by surface coating strategies. Polymer-coated bioceramic scaffolds can be simply produced by a dipping method that involves the immersion of the porous bioceramic in a polymer solution followed by drying in air. In this way, significant improvements in the compressive strength [132, 133, 134] as well as the fracture toughness can be obtained [135, 136].

Glass-ceramic scaffolds coated with the natural-derived polymer melanin, extracted from *Sepia officinalis* exhibited accelerated bioactivity, enhanced mechanical strength and local drug delivery ability, when compared with uncoated scaffolds [137]. Compressive strength increased from 0.5MPa to 1.3 MPa after melanin coating. The polymer coating covers the scaffolds struts and fills the microcracks present on the strut surface, improving the mechanical stability of the scaffold. The polymer reinforced the brittle glass-ceramic structure of struts increasing their toughness [137]. Uncoated scaffolds collapsed into powder during compressive test while the coated scaffolds partly retained their structure and did not collapse entirely. Polymer coating did not significantly affect the scaffolds' porosity. Vacuum assisted dip-coating method used for coating the scaffolds with the polymer solution decreased the porosity only slightly from 87.9% (uncoated scaffolds) to 87.1% (after coating) [137].

Polylactide-co-glycolide (PLGA) and 45S5 bioglass (BG) microspheres were used to fabricate porous PLGA-BG cylindrical scaffolds by heating the microspheres at 70 °C for 20 h in a stainless-steel mould [138]. PLGA-BG composite microspheres were formed through a water-oil-water emulsion, where PLGA granules were first dissolved in methylene chloride and then mixed with BG particles (<40 μm) and polyvinyl alcohol. The compressive strength of PLGA-BG composite scaffolds with a porosity of 43% was 0.42 ± 0.05MPa while the compressive modulus was 51.34 ± 6.08MPa. BG particles reinforced the polymeric matrix and provided bioactivity properties after immersion in simulated body fluid. Mechanical properties were tailored by controlling the polymer to bioactive glass ratio, co-polymer ratios, microsphere diameter, and sintering parameters (heating rate, temperature, and duration) [138].

PLA-HA scaffolds fabricated by electrospinning method showed improved mechanical strength compared to HA scaffolds. Scaffolds with high porosities (~97%) were fabricated

using the TIPS method. Pore morphology, microporosity, mechanical properties, bioactivity and degradation rates of TIPS can be controlled by varying the polymer concentration in the solution, volume fraction of secondary phase, quenching temperature and composition of solvent and polymers [139].

Polyethylene and polysulfone have been reported to be excellent polymeric matrices for the fabrication of composites including bioactive glass. Polysulfone is an amorphous polymer which has higher specific strength and modulus than polyethylene and could be used for load bearing prostheses [140].

Bioglass®/polysulfone composites have higher compressive modulus than the hydroxyapatite/polyethylene, Bioglass®/polyethylene and AW glass-ceramics/polyethylene composite systems (Table 4) [1, 2, 24, 25]. Specifically, the compressive modulus of Bioglass®/polysulfone composites with high glass content (Table 4) is close to the lower values of compressive modulus for human cortical bone. However, the synthetic composites generally fail to match the compressive modulus of natural bone, which may be due to the fact that the polymer/bioceramic interface is weak [24, 25]. This indicates that the interfacial strength between the bioceramic and polymer plays a key role that should be taken into account when designing and developing more effective bone-like composites.

Table 4 Mechanical properties of Bioglass®/polymer composite [141, 142, 143, 144]

Material	Volume of the bioceramic phase (%)	Compressive modulus (GPa)	Tensile strength (MPa)
Bioglass®/polyethylene	0	0.65	17.89
	10	1.05	14.34
	20	1.12	12.69
	40	2.54	10.75
Bioglass®/polysulfone	0	2.5	10.7
	20	4.65	2.5

	40	6.7	1.5
A-W glass ceramic/polyethylene	0	0.65	17.89
	10	0.96	17.32
	20	1.34	16.67
	30	1.83	14.68
	40	2.84	14.87

Polysulfone-45S5Bioglass composites were prepared by dissolving the polymer in chloroform, followed by mixing with Bioglass particles using different volume fraction and particles size [145, 146]. The polymer was then precipitated on the surface of the glass particles using ethanol. The resultant material was composed of well-distributed glass particles within a porous polymer matrix. The composite was then dried at 160 °C under vacuum for 12 h and hot pressed into a dense shape at 205 °C. Four-point bending tests of polysulfone-45S5Bioglass composites showed properties comparable with cortical bone. Mechanical properties depended on the volume fraction and particles size of Bioglass. Flexural strength varied between 50-80MPa, while flexural modulus was between 4-8GPa [145]. A four-point bending test was carried out on samples after immersion in a simulated body fluid at 37 °C for different periods of time up to 60 days [146]. The results showed a slow decrease of the flexural strength and flexural modulus after 35 days in the simulated fluid. The decrease of the mechanical properties (~20% for flexural strength and ~40% for flexural modulus) after simulated body fluid tests is related to glass dissolution due to ionic exchange process between the glass particles and fluid. Thus, fluid migration through the interface of the composite produces surface dissolution of glass particles and formation of voids, which are responsible for the decrease in mechanical properties [146].

10. Summary and discussion

To the best of the authors' knowledge, the last review paper specifically dedicated to the mechanical properties of bioactive glasses, ceramics and composites was published in 1998 by Thompson and Hench [147]. A bit surprisingly, no other "global" review has been published on this key topic over the past twenty years, although the mechanical behaviour of single classes of bioactive materials has been more recently discussed in a few specific papers [148, 149].

The present review aims to provide an up-to-date comprehensive picture as well as some comparisons among the different materials, which, now as then, are crucial and still challenging. Figure 8 illustrates the main material properties for load-bearing orthopaedic and dental applications. This includes the most relevant properties of fracture toughness, compressive strength and flexural strength for natural bone, dentine, enamel, alumina, zirconia, bioglass and calcium phosphate bioceramics. The graph was produced using CES EduPack 2018 software. The software database contains bulk values for these materials and does not include specific data for porous biomaterials, composites or hybrids. Nevertheless some interesting observations and comparisons can be made. Due to their mechanical properties, alumina and zirconia composites have been used for femoral head and acetabular cup components, while bioglasses and calcium phosphate bioceramics have typically been used for non-load bearing applications. As can be seen in Figure 8, calcium phosphate ceramics have fracture toughness * compressive strength values similar to transverse cortical bone and enamel, whilst the values of flexural strength are lower than those of cortical bone and dentine. Thus, calcium phosphates ceramics have been commercially used as coatings or incorporated in bone or dental cements. Bioglasses, alumina and zirconia have fracture toughness * compressive strength values which are higher than cortical bone, dentine and enamel. However, the flexural strength of bioglasses is lower than that of longitudinal

cortical bone. Alumina and zirconia have flexural strength values higher than cortical bone, dentine and enamel. Combined with their excellent wear resistance it is seen that only alumina and zirconia are currently used commercially for load bearing components such as hip and knee prostheses.

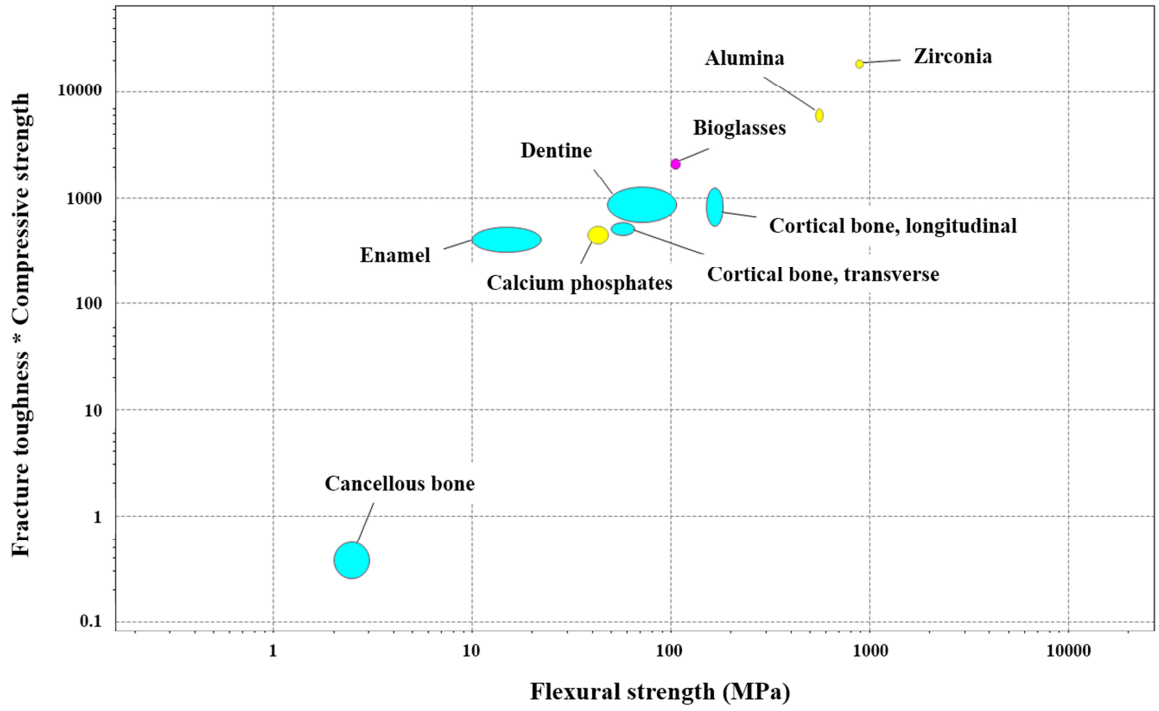

Figure 8 Fracture toughness (MPa • $m^{1/2}$) * compressive strength (MPa) versus flexural strength (MPa)

In modern tissue engineering approaches, however, there is often the need for processing bioactive materials in the form of 3D porous scaffolds that can support and direct the regeneration of newly-formed healthy tissue. This is a further challenge from both technological and mechanical viewpoints because (i) processing of glass or ceramic structures with suitable porosity for bone applications may not be an easy task and (ii) porosity obviously affects the mechanical performance.

The mechanical properties of bioactive glass or ceramic scaffolds can be improved by optimizing (i) the thermal processes (sintering) that are usually carried out to obtain the

material in a porous form and/or (ii) the material composition. The latter approach was particularly useful in the case of bioactive glasses: the tendency of 45S5 Bioglass to crystallize prior to achieving adequate densification pushed research towards the development of many other biomedical glasses with larger sinterability window, such as 13-93, which led to strong scaffolds with well-densified struts for potential use even in cortical bone repair [150].

Other interesting strategies to improve the mechanical properties of bioactive porous scaffolds involve the production of composites with polymeric phases or the application of a polymeric coating on the surface of the brittle struts/walls. The polymeric layer acts as a "glue" that holds the glass or ceramic particles together when the scaffold struts start to fail, thereby increasing both the compressive strength and toughness.

Bone, being a living tissue, exhibits the intrinsic ability to self-heal autonomously and continuously restore its mechanical performance, while synthetic implants do not possess these critical properties. However, bioactive hybrids allow moving a step towards this ideal "life-like" situation. Sol-gel hybrid materials are composed of interpenetrating networks of silicate and organic phases, which are able to intimately interact at the nanoscale and allow the material to behave as a single phase unlike "conventional" nanocomposites [151, 152]. This feature is responsible for highly controllable degradation rates, finely predictable mechanical performance and the capability of inducing spontaneous closing of cracks.

Technological advancement in the processing of powder-based bioactive glass and ceramic products is another key to improving mechanical performance. In this regard, additive manufacturing technology is regarded as a versatile class of fabrication methods for obtaining strong bioactive scaffolds even if intrinsically brittle MBGs are used [153]. Hence, hierarchical scaffolds with multifunctional capabilities (apatite-forming properties, controlled and local release of drugs/ions) can be successfully obtained.

Conclusions

Bioactive ceramics and glasses have been used for decades in the surgical repair of injured bone and teeth due to their biocompatibility and favourable physical and mechanical properties that are close to those of 'hard' tissues. However, the widespread use of these inorganic biomaterials, as well as their suitability for load-bearing applications, is still limited by their inherent brittleness and low fracture toughness (typically below 2MPa $m^{1/2}$). With designs inspired by those of biological structures that can be found in nature, such as cortical bone, glass-ceramics and bioceramic/polymer composites have demonstrated great potential for improving both strength and toughness compared to the 'parent' glasses used alone. Future research in the field of bone repair should focus on the development of more effective processing strategies (e.g. additive manufacturing) that allow optimizing the structure towards bioinspired, bone-like solutions. Furthermore, emerging applications of bioceramics and glasses in contact with soft tissues (e.g. wound healing, nerve repair, ocular implants) will require partial rethinking of biomechanical issues and optimizing the stiffness to match the compliance of delicate collagenous tissues.

Acknowledgements

GK is thankful to University Grant Commission (UGC) under the letter no. F.15/2013-2014/PDFWM-2013-2014-GE-PUN-14803 (SA-II) for providing financial assistance.

REFERENCES

1 G. Kaur, Bioactive glasses: Potential biomaterials for future therapy, Springer, Heidelberg, 2017

2 G. Kaur, O.P. Pandey, K. Singh, D. Homa, B. Scott, G. Pickrell, A review of bioactive glasses: Their structure, properties, fabrication, and apatite formation, Journal of Biomedical Material Research A 102 (2013), 254 – 274

3 DF Williams, Definitions in Biomaterials. Progress in Biomedical Engineering, Elsevier, Amsterdam, 1987

4 LL Hench, JK West, The sol-gel process, Chemical Reviews 90 (1990), 33-72

5 LL Hench, J Wilson, Introduction to Bioceramics, World Scientific, Singapore, 1993

6 LL Hench, JM Polak, Third generation Biomaterials, Science, 295 (2002), 1014

7 LL Hench, RJ Splinter, WC Allen, TK Greenlee, Bonding mechanisms at the interface of ceramic prosthetic materials, Journal of Biomedical Material Research 2 (1972), 117–141

8 LL Hench, Biomaterials: a forecast for the future, Biomaterials 19 (1998), 1419–1423

9 G. Kaur, G. Pickrell, N. Sriranganathan, V. Kumar, D. Homa, Review and the state of the art: Sol-gel or melt quenched bioactive glasses for tissue engineering, Journal of Biomedical Material Research: B Applied Biomaterials, 104 (6) (2016), 1248-75

10 D. Arcos, M. V. Regi, Sol–gel silica-based biomaterials and bone tissue regeneration, Acta Biomaterialia, 6 (2010) 2874–2888

11 T Albrektsson, C Johansson, Osteoinduction, osteoconduction and osseointegration, European Spine Journal 10 (2001), S96–101

12 R Shah, ACM Sinanan, JC Knowles, NP Hunt, MP Lewis, Craniofacial muscle engineering using a 3-dimensional phosphate glass fibre construct, Biomaterials 26 (2005), 1497–1505

13 QZ Chen, SE Harding, NN Ali, AR Lyon, A Boccaccini, Biomaterials in cardiac tissue engineering: ten years of research survey, Materials Science and Engineering R: Reports 59 (2008), 1–37

14 H Shin, S Jo, AG Mikos, Biomimetic materials for tissue engineering, Biomaterials 24 (2003), 4353–4364

15 S Minardi, B Corradetti, F Taraballi, et al., Evaluation of the osteoinductive potential of a bio-inspired scaffold mimicking the osteogenic niche for bone augmentation, Biomaterials 62 (2015), 128–37

16 P Ducheyne, Q Qiu, Bioactive ceramics: the effect of surface reactivity on bone formation and bone cell function, Biomaterials 20 (1999), 2287–2303

17 H H Lu, S F El-Amin, K D Scott, C T Laurencin, Three-dimensional, bioactive, biodegradable, polymer-bioactive glass composite scaffolds with improved mechanical

properties support collagen synthesis and mineralization of human osteoblast-like cells in vitro, Journal of Biomedical Material Research 64A (2003), 465–474

18 S S Kim, K M Ahn, M S Park, J H Lee, C Y Choi, B S Kim, A poly(lactide coglycolide)/ hydroxyapatite composite scaffold with enhanced osteoconductivity, Journal of Biomedical Material Research 80A (2007), 206–215

19 RM Day, AR Boccaccini, S Shurey, JA Roether, A Forbes, LL Hench, S Gabe, Assessment of polyglycolic acid mesh and bioactive glass for soft tissue engineering scaffolds, Biomaterials 25 (2004), 5857–5866

20 D Tomas, S Saroash, H R Graham, Apatite Glass-Ceramics: A Review, Frontiers in Materials 3 (2017) article 59

21 M C. Crovace, M T. Souza, C R. Chinaglia, O Peitl, E D. Zanotto, Biosilicate® - A multipurpose, highly bioactive glass-ceramic. In vitro, in vivo and clinical trials, Journal of Non-Crystalline Solids 432 (2016) 90–110

22 Min Wang, chapter 1.3 Bioactive glasses and glass-ceramics in: D. Shi (editor), Biomaterials and Tissue Engineering, Springer-Verlag Berlin Heidelberg New York 2004, pp 27-40

23 CES Edupack software 2018, Granta Design

24 J Park, Bioceramics : Properties, Characterizations, and Applications, Springer 2008

25 M N. Rahaman, D E. Day, B. S Bal, Q Fu, S B. Jung, L F. Bonewald, A P. Tomsia, Bioactive glass in tissue engineering, Acta Biomaterialia 7 (2011), 2355–2373

26 TV Thamaraiselvi, S Rajeswari, Biological Evaluation of Bioceramic Materials - A Review. Trends in Biomaterials and Artificial Organs 18 (2004), 9-17

27 J Chevalier, L Gremillard, Ceramics for medical applications: A picture for the next 20 years, Journal of the European Ceramic Society 29 (2009) 1245–1255

28 F. Baino, S. Hamzehlou, S. Kargozar. Bioactive glasses: where are we and where are we going? J Funct Biomater 2018;9:25

29 Hugo R. Fernandes, Anuraag Gaddam, Avito Rebelo, Daniela Brazete, George E. Stan, José M.F. Ferreira, Bioactive glasses and glass-ceramics for health care applications in bone regeneration and tissue engineering. *Materials* 2018, *11*, 2530

30 K Rezwan, QZ Chen, JJ Blaker, AR. Boccaccini, Biodegradable and bioactive porous polymer/inorganic composite scaffolds for bone tissue engineering, Biomaterials 27 (2006), 3413-3431

31 LG Griffith, Emerging design principles in biomaterials and scaffolds for tissue engineering, Annals of the New York Academy of Sciences 961 (2002), 83–95

32 QZ Chen, K Rezwan, D Armitage, SN Nazhat, AR Boccaccini, The surface functionalization of 45S5 Bioglass®-based glass-ceramic scaffolds and its impact on bioactivity, Journal of Materials Science: Materials in Medicine 17(11), 2006, 979-987

33 T. Kokubo, S. Ito, M. Shigematsu, S. Sakka, T. Yamamuro, Fatigue and life-time of bioactive glass-ceramic A-W containing apatite and wollastonite, Journal of Materials Science 22 (11) 1987, 4067-4070

34 T Kokubo, HM Kim, M Kawashita, Novel bioactive materials with different mechanical properties, Biomaterials 24 (2003) 2161–2175

35 E. Apel, J. Deubener, A. Bernard, M. Holand, R. Muller, H. Kappert, V. Rheinberger, W. Holand, Phenomena and mechanisms of crack propagation in glass-ceramics, Journal of the Mechanical Behavior of Biomedical Materials 1 (4), 2008, 313-325

36 M. Montazerian, E.D. Zanotto, History and trends of bioactive glass-ceramics, J. Biomed. Mater. Res. A 104 (2016) 1231–1249

37 L L. Hench, J R. Jones, Bioactive Glasses: Frontiers and Challenges, Frontiers in Bioengineering and Biotechnology 3 (2015) article 194

38 I. D. Thompson, L. L. Hench, Mechanical properties of bioactive glasses, glass-ceramics and composites, Proceedings of the Institution of Mechanical Engineers, Part H: Journal of Engineering in Medicine (Proc Inst Mech Eng H) 212(2) 1998, 127-136

39 O Peitl, GP LaTorre, LL Hench, Effect of crystallization on apatite layer formation of bioactive glass 45S5, Journal of Biomedical Material Research 30 (1996) 509–514

40 V.K. Marghussian, A. Sheikh-Mehdi Mesgar, Effects of composition on crystallization behaviour and mechanical properties of bioactive glass-ceramics in the MgO-CaO-SiO2-P2O5 system, Ceramics International 26 (2000) 415-420

41 M. U. Hashmi, S A. Shah, M. J. Zaidi, S. Alam, Effect of different CaO/MgO ratios on the structural and mechanical properties of bioactive glass-ceramics, Ceramics – Silikáty 56 (4) 2012, 347-351

42 A Mirza, M Riaz, R Zia, T Hussain, F Bashir, Effect of temperature on mechanical and bioactive properties of glass-ceramics, Journal of Alloys and Compounds 726 (2017) 348-351

43 J Al-Haidary1, M Al-Haidari, S Qrunfuleh, Effect of yttria addition on mechanical, physical and biological properties of ioactive MgO–CaO–SiO_2–P_2O_5–CaF_2 glass ceramic, Biomedical Materilas 3 (2008) 015005 (5pp)

44 VK Vyas et al, Assessment of nickel oxide substituted bioactive glass-ceramic on in vitro bioactivity and mechanical properties, Boletín de la sociedad española de cerámica y vidrio 55 (2016) 228–238

45 H.C. Li, D.G. Wang, X.G. Meng, C.Z. Chen, Effect of ZrO_2 additions on the crystallization, mechanical and biological properties of MgO–CaO–SiO_2–P_2O_5–CaF_2 bioactive glass-ceramics, Colloids and Surfaces B: Biointerfaces 118 (2014) 226–233

46 MN Rahaman, A Yao, Bal B Sonny, JP Garino, MD Ries, Ceramics for prosthetic hip and knee joint replacement, Journal of the American Ceramic Society 90 (2007), 1965-1988

47 S Ramakrishna, J Meyer, E Wintermantel, KW Leong, Biomedical applications of polymer-composite materials: a review, Composites Science and Technology 61(2001) 1189-1224

48 DF Williams, Consensus and definitions in biomaterials, Advances in Biomaterials, Elsevier Science, Amsterdam, 1988, p. 11-16

49 LL Hench, Bioceramics: from concept to clinic, Journal of the American Ceramic Society 74 (1991), 1487–1510

50 J.J Webster, L.W Siegel, R Bizios, An in vitro evaluation of nanophase alumina for orthopaedic /dental applications, in R.Z Lolesss, J.P Lelyernc (Eds.), Bioceramics: Proceedings of the 11th International symposium on ceramics in Medicine, World Scientific, New York, 1998, pp. 273

51 Calcium orthophosphates ($CaPO_4$): occurrence and properties

52 Nanostructured Calcium Phosphates: Preparation and Their Application in Biomedicine

53 Y.H. Hsu, I.G. Turner, A.W. Miles, Mechanical properties of three different compositions of calcium phosphate bioceramic following immersion in Ringer's solution and distilled water, Journal of Materials Science: Materials in Medicine 20 (2009), 2367–2374

54 E. M. Carlisl, Silicon: a possible factor in bone calcification. Science, 167 (1970), 279–80.

55 K. Schwarz, A bound form of silicon in glycosaminoglycans and polyuronides Proc. Natl Acad. Sci. USA 70 (1973), 1608–12

56 S. Padilla, J. Roman, S. Sanchez-Salcedo and M. Vallet-Regi, Hydroxyapatite/SiO(2)-CaO-P(2)O(5) glass materials: in vitro bioactivity and biocompatibility. Acta Biomater. 2 (2006), 331–42

57 F. Balas, J. Perez-Pariente and M. Vallet-Regi, In vitro bioactivity of silicon-substituted hydroxyapatites. J. Biomed. Mater. Res. A 66 (2003), 364–75

58 C. Wu and J. Chang, A review of bioactive silicate ceramics, Biomed. Mater. 8 (2013) 032001

59 Y. Huang, X. Jin, X. Zhang, H. Sun, J. Tu, T. Tang, J. Chang and K. Dai, In vitro and in vivo evaluation of akermanite bioceramics for bone regeneration. Biomaterials 30 (2009), 5041–8

60 L. Xia, Z. Zhang, L.Chen, W. Zhang, D. Zeng, X. Zhang, J. Chang and X. Jiang, Proliferation and osteogenic differentiation of human periodontal ligament cells of akermanite and beta-TCP bioceramics. Eur. Cell Mater. 22 (2011), 68–82

61 C. Wu and J. Chang, Silicate bioceramics for bone tissue regeneration. J. Inorg. Mater. 28 (2013), 29–39

62 P.N. De Aza, Z.B. Luklinska, M.R. Anseau, F. Guitian and S. De Aza, Transmission electron microscopy of the interface between bone and pseudowollastonite implant. J. Microsc. 201(2001), 33–43.

63 S. Xu, K. Lin, Z. Wang, J. Chang, L. Wang, J. Lu and C. Ning,2008 Reconstruction of calvarial defect of rabbits using porous calcium silicate bioactive ceramics. Biomaterials, 29 (2008), 2588–96

64 X.G. Jin, J.A. Chang, W.Y. Zhai and K.L. Lin, Preparation and characterization of clinoenstatite bioceramics. J. Am. Ceram. Soc. 94 (2011), 173–7.

65 F. Tavangarian and R. Emadi, Nanostructure effects on the bioactivity of forsterite bioceramic. Mater. Lett. 65 (2011), 740–3

66 C. Wu and J. Chang, Synthesis and in vitro bioactivity of bredigite powders. J. Biomater. Appl. 21 (2007), 251–63.

67 Y. Ramaswamy, C. Wu, C.R. Dunstan, B. Hewson, T. Eindorf, G.I. Anderson and H. Zreiqat, Sphene ceramics for orthopedic coating applications: an in vitro and in vivo study. Acta Biomater. 5 (2009), 3192–204.

68 W. Lu, W. Duan, Y. Guo and C. Ning, Mechanical properties and in vitro bioactivity of Ca5(PO4)2SiO4 bioceramic. J Biomater. Appl. 26 (2010), 637–50.

69 H. Zreiqat, Y. Ramaswamy, C. Wu, A. Paschalidis, Z. Lu, B. James, O. Birke, M. McDonald, D. Little and C.R. Dunstan, The incorporation of strontium and zinc into a calcium-silicon ceramic for bone tissue engineering. Biomaterials 31(2010), 3175–84.

70 C. Wu and J. Chang, A novel akermanite bioceramic: preparation and characteristics. J. Biomater. Appl. 21(2006), 119–29.

71 K.L. Lin, W.Y. Zhai, S.Y. Ni, J. Chang, Y. Zeng and W.J. Qian, Study of the mechanical property and in vitro biocompatibility of CaSiO3 ceramics. Ceram. Int. 31 (2005), 323–6

72 Microstructure, mechanical properties and in vitro bioactivity of akermanite scaffolds fabricated by laser sintering, Biomedical Materials and Engineering 24 (2014) 2073–2080 2073 DOI 10.3233/BME-141017 IOS.

73 H.B. Zhong, L.J.Wang, Y.C. Fan, L.F. He, K.L. Lin, W. Jiang, J. Chang and L.D. Chen, Mechanical properties and bioactivity of beta-Ca_2SiO_4 ceramics synthesized by spark plasma sintering. Ceram. Int. 37 (2011), 2459–65

74 S Ni, J Chang, L Chou, In vitro studies of novel CaO-SiO2-MgO system composite bioceramics, Journal of Materials Science: Materials in Medicine 19 (1), 2008, 359-67

75 H Liu, T J Webster, Nanomedicine for implants: a review of studies and necessary experimental tools Biomaterials 28 (2007), 354–69

76 HW Kim, JC Knowles, HE Kim, Hydroxyapatite porous scaffold engineered with biological polymer hybrid coating for antibiotic vancomycin release, Journal of Materials Science: Materials in Medicine 16 (2005), 189–95

77 M. Kharaziha, M.H. Fathi, Improvement of mechanical properties and biocompatibility of forsterite bioceramic addressed to bone tissue engineering materials, Journal of the Mechanical Behaviour of Biomedical Materials 3(2010) 530–537

78 M. Kharaziha, M.H. Fathi, Synthesis and characterization of bioactive forsterite nanopowder, Ceramics International 35 (2009) 2449–2454

79 S Ni, L Chou, J Chang, Preparation and characterization of forsterite (Mg2SiO4) bioceramics, Ceramics International 33 (2007), 83–88

80 B A. Allo, D O. Costa, S. J Dixon, K Mequanint, A S. Rizkalla, Bioactive and Biodegradable Nanocomposites and Hybrid Biomaterials for Bone Regeneration, Journal of Functional Biomaterials 3 (2012) 432-463

81 D Mondal, S. J Dixon, K Mequanint, A S. Rizkalla, Mechanically-competent and cytocompatible polycaprolactone-borophosphosilicate hybrid biomaterials, Journal of the Mechanical Behavior of Biomedical Materials 75 (2017) 180–189

82 J J. Chung, S Li, M M. Stevens, T K. Georgiou, J R. Jones, Tailoring Mechanical Properties of Sol–Gel Hybrids for Bone Regeneration through Polymer Structure, Chemistry of Materials 28 (2016), 6127−6135

83 S-H Rhee, Bone-like apatite-forming ability and mechanical properties of poly(ε-caprolactone) / silica hybrid as a function of poly(ε-caprolactone) content, Biomaterials 25 (2004) 1167–1175

84 F A Dourbash, P Alizadeh, S Nazari, A Farasat, A highly bioactive poly (amido amine)/70S30C bioactive glass hybrid with photoluminescent and antimicrobial properties for bone regeneration, Materials Science and Engineering C 78 (2017) 1135–1146

85 Tadashi Kokubo, Hyun-Min Kim, Masakazu Kawashita, Novel bioactive materials with different mechanical properties, Biomaterials 24 (2003) 2161–2175

86 Q Chen, F Miyaji, T Kokubo, T Nakamura, Apatite formation on PDMS-modified CaO-SiO_2-TiO_2 hybrids prepared by sol-gel process, Biomaterials 20 (1999) 1127-1132

87 Q Chen, N Miyata, T Kokubo, T Nakamura, Effect of heat treatment on bioactivity and mechanical properties of PDMS modified CaO-SiO_2-TiO_2 hybrids via sol-gel process, Journal of Materials Science: Materials in Medicine 12 (2001) 515–522

88 M Kamitakahara, M Kawashita, N Miyata, T Kokubo, Bioactivity and mechanical properties of polydimethylsiloxane (PDMS)-CaO-SiO_2 hybrids with different PDMS contents, Journal of Sol-Gel Science and Technology 21 (2001) 75–81.

89 M Kamitakahara, M Kawashita, N Miyata, T Kokubo, Bioactivity and mechanical properties of polydimethylsiloxane (PDMS)-CaO-SiO_2 hybrids with different calcium contents, Journal of Materials Science: Materials in Medicine 13 (2002) 1015–1020

90 T Miyazaki, H Akita, E Ishida, M Ashizuka, C Ohtsuki, Synthesis of bioactive organic-inorganic hybrids from tetraisopropyl titanate and hydroxyethyl methacrylate, Journal of the Ceramic Society of Japan 114, issue 1325 (2006) 87-91

91 K. Tsuru, C. Ohtsuki, A. Osaka, Bioactivity of sol–gel derived organically modified silicates. Part I: In vitro examination, Journal of Materials Science: Materials in Medicine 8 (1997) 157-161

92 T. Yabuta, E.P. Bescher, J.D. Mackenzie, K. Tsuru, S. Hayakawa, A. Osaka, Synthesis of PDMS-Based Porous Materials for Biomedical Applications, Journal of Sol-Gel Science and Technology 26 (2003), 1219–1222

93 Q Chen, N Miyata, T Kokubo, T Nakamura, Bioactivity and mechanical properties of PDMS-modified CaO–SiO2–TiO2 hybrids prepared by sol-gel process, Journal of Biomedical Materials Research, 51 (4), 2000, 605–611

94 Y Aburatani, K Tsuru, S Hayakawa, A Osaka, Mechanical properties and microstructure of bioactive ORMOSILs containing silica particles, Materials Science and Engineering C 20 (2002) 195–198

95 X Zhao, Y Wu, Y Du, X Chen, B Lei, Y Xue, P X. Ma, A highly bioactive and biodegradable poly(glycerol sebacate)–silica glass hybrid elastomer with tailored mechanical properties for bone tissue regeneration, Journal of Materials Chemistry B 3 (2015) 3222-3233

96 Francesca Tallia, Laura Russo, Siwei Li, Alexandra L. H. Orrin, Xiaomeng Shi, Shu Chen, Joseph A. M. Steele, Sylvain Meille, Jérôme Chevalier, Peter D. Lee, Molly M. Stevens, Laura Cipolla, Julian R. Jones, Bouncing and 3D printable hybrids with self-healing properties. Mater. Horiz., 2018,5, 849-860

97 V Karageorgiou, D Kaplan, Porosity of 3D biomaterial scaffolds and osteogenesis. Biomaterials 26 (2005), 5474–5491

98 KA Hing, Bioceramic bone graft substitutes: influence of porosity and chemistry, International Journal of Applied Ceramic Technology 2 (2005), 184-199

99 E. Fiume, J. Barberi, E. Verné, F. Baino. Bioactive glasses: from parent 45S5 composition to scaffold-assisted tissue-healing therapies. J Funct Biomater 2018;9:24

100 J. Massera, S. Fagerlund, L-. Hupa, M. Hupa, Crystallization mechanism of the bioactive glasses, 45S5 and S53P4, J. Am. Ceram. Soc. 95 (2012) 607–613

101 F. Baino, E. Fiume. Quantifying the effect of particle size on the crystallization of 45S5 bioactive glass. Mater Lett 2018;224:54-58

102 O. Peitl, E.D. Zanotto, L.L. Hench, Highly bioactive P2O5–Na2O–CaO–SiO2 glassceramics, J. Non-Cryst. Solids 292 (2001) 115–126

103 H. Arstila, L. Hupa, K. Karlson, M. Hupa, In vitro bioactivity of partially crystallised glasses, Glass Technol. Eur. J. Glass Sci. Technol. A 48 (2007) 196–199

104 Q.Z. Chen, I.D. Thompson, A.R. Boccaccini, 45S5 Bioglass-derived glass-ceramic scaffolds for bone tissue engineering, Biomaterials 27 (2006) 2414–2425

105 S Xu, X Yan, X Chen, H Shao, Y He, L Zhang, G Yang, Z Gou, Effect of borosilicate glass on the mechanical and biodegradation properties of 45S5-derived bioactive glass-ceramics Journal of Non-Crystalline Solids 405 (2014) 91–99

106 X. Yang, L. Zhang, X. Chen, X. Sun, G. Yang, X. Guo, H. Yang, C. Gao, Z. Gou, Influence of B2O3 on the thermal and bioactive properties of CaO–SiO2–P2O5 system, Journal of Non-Crystalline Solids 358 (2012) 1171–1179

107 Q. Yang, S Chen, H. Shi, H Xiao, Y Ma, In vitro study of improved wound-healing effect of bioactive borate-based glass nano-/micro-fibers, Materials Science and Engineering C 55 (2015), 105–117

108 F Baino, M Ferraris, O Bretcanu, E Verné, C Vitale-Brovarone, Optimization of composition, structure and mechanical strength of bioactive 3-D glass-ceramic scaffolds for bone substitution, Journal of Biomaterials Applications 27(7) 2013, pp. 872-890

109 KW Dalgarno, DJ Wood, RD Goodridge, K Xiao, C Ohtsuki, P Genever, J Dyson, Mechanical properties and biological responses of bioactive glass ceramics processed using indirect SLS, 16th Solid Freeform Fabrication Symposium, Austin, Texas, United States, SFF (2005), 132-140

110 K.L. Lin, J. Chang, Y. Zeng and W.J. Qian, Preparation of macroporous calcium silicate ceramics. Mater. Lett.58 (2004), 2109–130

111 P. Miranda, A. Pajares, E. Saiz, A.P. Tomsia and F. Guiberteau, Mechanical properties of calcium phosphate scaffolds fabricated by robocasting. J. Biomed. Mater. Res. A 85(2008), 218–27

112 P. Miranda, E. Saiz, K. Gryn and A.P. Tomsia, Sintering and robocasting of beta-tricalcium phosphate scaffolds for orthopaedic applications. Acta Biomater. 2(2006), 457–66.

113 C.T. Wu, W. Fan, Y.H. Zhou, Y.X. Luo, M. Gelinsky, J. Chang and Y. Xiao, 3D-printing of highly uniform $CaSiO_3$ceramic scaffolds: preparation, characterization and in vivo osteogenesis. J. Mater. Chem. 22(2012), 12288–95

114 Yang Yu, Zoltán Bacsik, Mattias Edén. Contrasting *In Vitro* Apatite Growth From Bioactive Glass Surfaces with that of Spontaneous Precipitation. Materials 2018, 11, 1690

115 F. Baino. Bioactive glasses - when glass science and technology meet regenerative medicine. Ceram Int 2018;44:14953-14966

116 A Nommeots-Nomm, P D. Lee, J R. Jones, Direct ink writing of highly bioactive glasses, Journal of the European Ceramic Society 38 (2018) 837–844

117 X Liu, M N. Rahaman, G E. Hilmas, B. S Bal, Mechanical properties of bioactive glass (13-93) scaffolds fabricated by robotic deposition for structural bone repair, Acta Biomaterialia 9 (2013) 7025–7034

118 K C.R. Kolan, M C. Leu, G E. Hilmas, R F Brown, M Velez, Fabrication of 13-93 bioactive glass scaffolds for bone tissue engineering using indirect selective laser sintering, Biofabrication 3 (2011), 025004

119 K C.R. Kolan, M C. Leu, G E. Hilmas, M Velez, Effect of material, process parameters, and simulated body fluids on mechanical properties of 13-93 bioactive glass porous constructs made by selective laser sintering, Journal of the Mechanical Behavior of Biomedical Materials 13 (2012) 14-24

120 Q Fu, M N. Rahaman, B. S Bal, R F. Brown, D E. Day, Mechanical and in vitro performance of 13–93 bioactive glass scaffolds prepared by a polymer foam replication technique, Acta Biomaterialia 4 (2008) 1854–1864

121 E. Fiume, E. Verné. F. Baino. Crystallization behavior of SiO_2-P_2O_5-CaO-MgO-Na_2O-K_2O bioactive glass powder. Biomed Glasses 2019;5:46-52

122 Q Fu, F. Baino, J. Barberi, E. Fiume, G. Orlygsson, J. Massera, E. Verné. Robocasting of bioactive SiO_2-P_2O_5-CaO-MgO-Na_2O-K_2O glass scaffolds. J Healthcare Eng 2019;2019:Article ID 5153136

123 C. Wu, W. Fan, M. Gelinsky, Y. Xiao, P. Simon, R. Schulze, T. Doert, Y. Luo and G. Cuniberti, Bioactive SrO-SiO(2) glass with well-ordered mesopores: characterization, physiochemistry and biological properties. Acta Biomater.7 (2011), 1797–806

124 S. Kargozar, M. Montazerian, S. Hamzehlou, H.W. Kim, F. Baino. Mesoporous bioactive glasses: promising platforms for antibacterial strategies. Acta Biomater 2018;81:1-19

125 F. Baino, E. Fiume, M. Miola, E. Verné. Bioactive sol-gel glasses: processing, properties, and applications. Int J Appl Ceramic Technol 2018;15:841-860

126 D. Arcos, M. Vallet, Regi, Sol–gel silica-based biomaterials and bone tissue regeneration, Acta Biomater. 6 (2010) 2874–2888

127 Wu C, Zhang Y, Zhu Y, Friis T, Xiao Y. Structure-property relationships of silk-modified mesoporous bioglass scaffolds. *Biomaterials* 31, 3429-3438 (2010).

128 Wu C, Luo Y, Cuniberti G, Xiao Y, Gelinsky M. Three-dimensional printing of hierarchical and tough mesoporous bioactive glass scaffolds with a controllable pore architecture, excellent mechanical strength and mineralization ability. *Acta Biomater.* 7, 2644-2650 (2011)

129 Zhang J, Zhao S, Zhu Y, Huang Y, Zhu M, Tao C, Zhang C. Three-dimensional printing of strontium-containing mesoporous bioactive glass scaffolds for bone regeneration. *Acta Biomater.* 10, 2269-2281 (2014).

130 E. Salernitano, C. Migliaresi, Composite materials for biomedical applications: a review, Journal of Applied Biomaterials & Biomechanics 1 (2003), 3-18

131 Q Fu, E Saiz, M N. Rahaman, A P. Tomsia, Bioactive glass scaffolds for bone tissue engineering: state of the art and future perspectives, Materials Science and Engineering C 31 (2011) 1245–1256

132 D.M Yunos, O.Bretcanu, A Boccaccini, Polymer-bioceramic composites for tissue engineering scaffolds, Journal of Materials Science: Materials in Medicine 43 (2008), 4433-4442

133 O Bretcanu, Q Chen, S. K Misra, A. R Boccaccini, E Verné, C Vitale- Brovarone, Biodegradable polymer coated 45S5 bioglass-derived glass-ceramic scaffolds for bone tissue engineering, Glass Technology: European Journal of Glass Science and Technology Part A 48 (2007), 227–234

134 O Bretcanu, S Misra, I Roy, C Renghini, F Fiori, AR Boccaccini, V Salih, In vitro biocompatibility of 45S5 Bioglass®-derived glass-ceramic scaffolds coated with poly(3-hydroxybutyrate), Journal of Tissue Engineering and Regenerative Medicine 3 (2), 2009, Pages 139-148

135 O Bretcanu, A R. Boccaccini, V Salih, Poly-DL-lactic acid coated Bioglass® scaffolds: toughening effects and osteosarcoma cell proliferation, Journal of Materials Science 47 (2012), 5661–5672

136 L Rehorek, Z Chlup, D Meng, D M Yunos, A. R Boccaccini, I Dlouhy, Response of 45S5 bioglass® foams to tensile loading, Ceramics International 39 (2013), 8015–8020

137 M. Araújo, R. Viveiros, A. Philippart, M.Miola, S. Doumett, G. Baldi, J. Perez, A.R. Boccaccini, A. Aguiar-Ricardo, E. Verné, Bioactivity, mechanical properties and drug delivery ability of bioactive glass-ceramic scaffolds coated with a natural-derived polymer, Materials Science and Engineering C 77 (2017) 342–351

138 H H. Lu, S F. El-Amin, K D. Scott, C T. Laurencin, Three-dimensional, bioactive, biodegradable, polymer–bioactive glass composite scaffolds with improved mechanical properties support collagen synthesis and mineralization of human osteoblast-like cells in vitro, J Biomed Mater Res 64A (2003), 465–474

139 S Tajbakhsh, F Hajiali, A comprehensive study on the fabrication and properties of biocomposites of poly(lactic acid)/ceramics for bone tissue engineering, Materials Science and Engineering C 70 (2017) 897–912

140 M Wang, Developing bioactive composite materials for tissue replacement, Biomaterials 24 (2003) 2133–2151

141 R G. Kaur (Editor), Clinical Applications of Biomaterials: State-of-the-art progress, trends and novel approaches"- Springer (New York, USA), ISBN 978-3-319-56059-5

142 M. Wang, W. Bonfield, and L. L. Hench, BioglassA/high density polyethylene composite as a new soft tissue bonding material. In Bioceramics (Eds J. Wilson, L. L. Hench and D. G. Greenspan), Vol. 8 (Pergamon, Florida, USA).

143 W. Bonfield, et al. Hydroxyapatite reinforced polyethylene-a mechanically compatible implant. Biomaterials, 1981, 2, 185

144 R. L. Orefice, G. P. LaTorre, J. K. West, and L. L. Hench, Processing and characterisation of bioactive polysulphone BioglassA composites. In Bioceramics (Eds J. Wilson, L. L. Hench and D. G. Greenspan), Vol. 8 (Pergamon, Florida, USA)

145 R Orefice, A Clark, J West, A Brennan, L Hench, Processing, properties, and in vitro bioactivity of polysulfone-bioactive glass composites, Journal of Biomedical Materials Research 80A (2007), 565–580

146 R Orefice, J West, G LaTorre, L Hench, A Brennan, Effect of Long-Term In Vitro Testing on the Properties of Bioactive Glass-Polysulfone Composites, Biomacromolecules 11 (2010), 657–665.

147 Thompson JD, Hench LL. Mechanical properties of bioactive glasses, glass-ceramics and composites. Proc Inst Mech Eng H J Eng Med 1998;212:127–136

148 Q. Fu, E. Saiz, A.P. Tomsia, Bioinspired strong and highly porous glass scaffolds, Adv. Funct. Mater. 21 (2011) 1058–1063

149 Siddiqui HA, Pickering KL, Mucalo MR. A Review on the Use of Hydroxyapatite-Carbonaceous Structure Composites in Bone Replacement Materials for Strengthening Purposes, Materials 2018, 11, 1813

150 MN Rahaman, W Xian, W Huang. Review - bioactive glass implants for potential application in structural bone repair. Biomed Glasses 2017, 3, 56-66

151 Valliant, E.M.; Jones, J.R. Softening bioactive glass for bone regeneration: sol-gel hybrid materials. Soft Matter **2011**, 7, 5083–5095

152 F. Baino, S. Fiorilli, C. Vitale-Brovarone. Composite biomaterials based on sol-gel mesoporous silicate glasses: a review. Bioengineering 2017;4:15

153 Hongshi Ma, Chun Feng, Jiang Chang, Chengtie Wu. 3D-printed bioceramic scaffolds: From bone tissue engineering to tumor therapy. Acta Biomaterialia 79 (2018) 37–59